

# Effective pair potentials for spherical nanoparticles

**Ramses van Zon**

Chemical Physics Theory Group, Department of Chemistry, University of Toronto, 80 Saint George Street, Toronto, ON, M5S 3H6, Canada  
E-mail: [rzon@chem.utoronto.ca](mailto:rzon@chem.utoronto.ca)

Received 3 November 2008

Accepted 3 December 2008

Published 2 February 2009

Online at [stacks.iop.org/JSTAT/2009/P02008](http://stacks.iop.org/JSTAT/2009/P02008)

[doi:10.1088/1742-5468/2009/02/P02008](https://doi.org/10.1088/1742-5468/2009/02/P02008)

**Abstract.** An effective description for rigid spherical nanoparticles in a fluid of point particles is presented. The points inside the nanoparticles and the point particles are assumed to interact via spherically symmetric additive pair potentials, while the distribution of points inside the nanoparticles is taken to be spherically symmetric and smooth. The resulting effective pair interactions between a nanoparticle and a point particle, as well as between two nanoparticles, are then given by spherically symmetric potentials. If overlap between particles is allowed, as can occur for some forms of the pair potentials, the effective potential generally has non-analytic points. It is shown that for each effective potential the expressions for different overlapping cases can be written in terms of one analytic auxiliary potential. Even when only non-overlapping situations are possible, the auxiliary potentials facilitate the formulation of the effective potentials. Effective potentials for hollow nanoparticles (appropriate e.g. for buckyballs) are also considered and shown to be related to those for solid nanoparticles. For hollow nanoparticles overlap is more physical, since this covers the case of a smaller particle embedded in a larger, hollow nanoparticle. Finally, explicit expressions are given for the effective potentials derived from basic pair potentials of power law and exponential form, as well as from the commonly used London–van der Waals, Morse, Buckingham, and Lennard–Jones potentials. The applicability of the latter is demonstrated by comparison with an atomic description of nanoparticles with an internal face centered cubic structure.

**Keywords:** colloids, bio-colloids and nano-colloids

**ArXiv ePrint:** [0803.4186](https://arxiv.org/abs/0803.4186)

---

**Contents**

<b>1. Introduction</b>	<b>2</b>
<b>2. Smoothing procedure for nanoparticle potentials</b>	<b>3</b>
<b>3. Auxiliary potential formulation</b>	<b>7</b>
3.1. Effective potential between a point particle and a nanoparticle . . . . .	9
3.2. Effective potential between two nanoparticles . . . . .	10
3.3. Ambiguity in the auxiliary potentials . . . . .	12
<b>4. Solid and hollow nanoparticles</b>	<b>12</b>
<b>5. Effective potentials for uniformly solid and hollow nanoparticles</b>	<b>14</b>
5.1. Power laws . . . . .	14
5.2. Exponentials . . . . .	16
5.3. Examples using common pair potentials . . . . .	17
<b>6. Accuracy of Lennard-Jones-based potentials for fcc nanoparticles</b>	<b>23</b>
<b>7. Discussion</b>	<b>26</b>
<b>Acknowledgments</b>	<b>28</b>
<b>Appendix. The kernel <math>K_{ij}</math></b>	<b>28</b>
<b>References</b>	<b>29</b>

---

**1. Introduction**

Nanoparticles [1]–[3], quantum dots [4], (nano)colloidal suspensions [5, 6], and globular proteins [7, 8] are examples of physical systems in which small nanometer or micron-sized clusters of particles are suspended in a fluid. Such systems have applications ranging from material coatings to drug delivery [9, 10]. For colloidal systems, collective behavior has been the focus of much research [6, 11], while nanoclusters are often studied as isolated objects [12]–[16], despite interesting collective phenomena such as the increased heat conductance in dilute nanoparticle suspensions [2] and self-assembly [6].

To study the collective properties of nanoparticles in suspension, one would expect a detailed description of the internal structure of the clusters not to be necessary, especially if the nanoparticles are more or less solid. On the other hand, a description in terms of hard spheres would probably be too crude for nanoparticles since typical atomic interaction ranges are on the order of ångströms. The main goal of this paper is to derive a general effective description of solid and hollow, rigid, spherical nanoparticles. The description will retain a level of detail beyond the hard sphere model and is intended to be used in the study of the collective behavior of nanoparticles, either numerically or analytically. The starting point of the description is to assume that each nanoparticle is composed of particles with fixed relative positions, interacting with the point particles in the fluid and their counterparts in other nanoparticles through spherically symmetric pair potentials. The nanoparticles' distribution of constituents is

modeled as a smooth spherically symmetric density, which can be viewed as a smoothing procedure for the interactions. Solid and hollow spheres of uniform density are considered in detail, since these are suitable for describing solid nanoclusters and buckyballs (or similar structures), respectively. The spherical smoothing procedure results in spherically symmetric effective interaction potentials for nanoparticles and point particles, and consequently leads to a description of nanoparticles as single particles instead of as collections of particles.

Similar approaches to the problem of constructing effective potentials for spherical particles have been used before, but only for specific cases [1], [14]–[21], while other effective potentials for nanoparticles have been simply posed ad hoc [7, 24, 25]. The current paper is devoted to the general method of deriving effective pair potentials for nanoparticles from the basic pair potential of their constituents, assuming spherical, rigid nanoparticles. The (spherical) cases treated in [1], [14]–[16], [18, 17], [19]–[21] are then special cases of the general formalism presented here.

Specific cases of non-spherical geometries have been considered in the literature, e.g., planes [17]–[19] and tubes in specific orientations (see [19] and references therein). However, the general treatment of effective interactions for non-spherical objects poses additional difficulties due to the orientational dependence of the interaction, with the exception of infinite planes, which can be viewed as limiting cases of spheres. For that reason, only spherical ones will be considered here.

The treatment is not restricted to non-overlapping particles (often the only physical possibility) but covers the possibility of overlapping and embedded particles as well, when allowed by the physics of the problem. For instance, within the formalism developed in this paper, a small particle embedded in a larger hollow sphere is considered to be an overlapping situation. Because the effective potentials for hollow nanoparticles are derived from those of solid nanoparticles, overlapping solid nanoparticles will also have to be considered, at least formally.

The paper is structured as follows. In section 2, the general smoothing procedure is explained. Properties of the resulting effective potentials are explored in section 3, with special consideration for the difference between non-overlapping and overlapping particles, which results in a reformulation of the non-analytic effective potentials in terms of analytic auxiliary potentials. In section 4, the formalism is extended to include hollow nanoparticles. For uniform solid and hollow nanoparticle structures, explicit effective potentials for a nanoparticle and a point particle and for different nanoparticles are worked out in section 5 for the London–van der Waals potential, the exponential potential, the Morse potential, the (modified) Buckingham potential, and the Lennard-Jones potential. Section 6 addresses the applicability of the effective potentials by comparison with an atom-based nanoparticle model. A discussion in section 7 concludes the paper.

## 2. Smoothing procedure for nanoparticle potentials

Consider a classical system of point particles, representing a fluid, and spherical clusters called nanoparticles. While in reality, a nanoparticle is a cluster of a number of atoms, here each nanoparticle will be modeled by a smooth internal density profile  $\rho(x)$  that depends on the distance  $x$  from the center of the nanoparticle only and which is strictly zero for  $x > s$ , where  $s$  is the radius of the spherical nanoparticle. This approximation

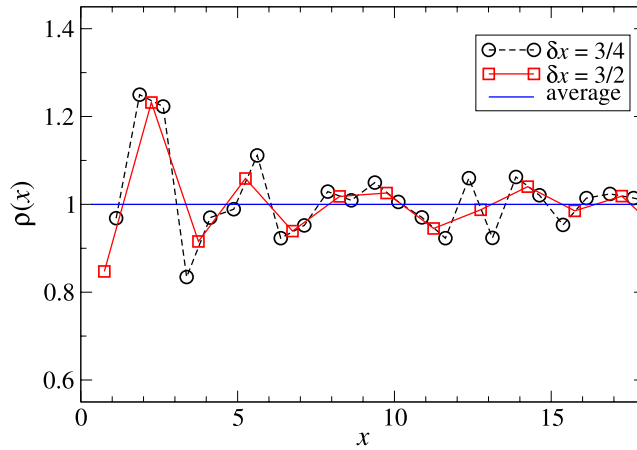


**Figure 1.** Coarse-grained radial density profile of the fcc lattice of mean density  $\bar{\rho} = 1$  as a function of the distance from a central atom. The circles correspond to a coarse-graining width of  $\delta x = 3/4$ , the squares correspond to  $\delta x = 3/2$  (the points are connected to guide the eye). The horizontal line indicates the mean number density.

is motivated by the idea that for spherical nanoparticles, the inhomogeneities due to the discreteness of the atoms inside the nanoparticles should only have a small influence on the effective nanoparticle potentials. Given a density profile  $\rho(x)$ , one can make contact with the picture of a nanoparticle as a cluster of distinct atoms by interpreting  $M = \int_{\mathcal{B}_s} d\mathbf{x} \rho(x)$  as the total number of atoms inside the nanoparticle, where  $x = |\mathbf{x}|$ , and  $\mathcal{B}_s$  denotes that the integration over  $\mathbf{x}$  is over the volume of a ball of radius  $s$  around zero.

To further illustrate that it is reasonable to smooth out the internal density, consider the idealized case where the atoms composing the nanoparticle are arranged in a face centered cubic (fcc) lattice—the crystal structure of e.g. aluminum, silver, gold, and platinum [22]—with one of the atoms in the center. The true density inside the nanoparticle is then a sum of delta functions, but this can be coarse-grained by taking a spherical shell of radius  $x$  with a width  $\delta x$ , counting the number of atoms in the shell, and dividing by the volume of the shell. The result of such coarse-graining is shown in figure 1 for a lattice with mean number density  $\bar{\rho} = 1$  and for two values of the coarse-graining width,  $\delta x = 3/4$  and  $3/2$ . The coarse-grained density around a single atom in an fcc crystal is seen to be reasonably constant except near the central atom, with the positive and negative deviations from the mean density averaging out for larger  $\delta x$ . Therefore, to first order, the density may be replaced by a constant. The actual applicability of this smoothing procedure depends of course on the relative length scales in the system. It is expected that the particles need to be at least several nanometers in size for the smoothing to be applicable, but this has to be tested. As a first step, the highly idealized fcc nanoparticles will therefore be used again in section 6 to get an idea of the accuracy of the effective potentials.

Let  $\phi_{\text{pn}}(r)$  denote the basic pair potential between a point of a nanoparticle and a point particle in the fluid, where  $r$  is the distance between them. This potential will be assumed to be analytic for  $r > 0$  but may diverge as  $r \rightarrow 0$  as is the case for many

phenomenological inter-atomic potentials. The effective point–nanoparticle pair potential  $V_{\text{pn}}$  is then given by

$$V_{\text{pn}}(r) = \int_{\mathcal{B}_s} d\mathbf{x} \rho(x) \phi_{\text{pn}}(|\mathbf{r} - \mathbf{x}|), \quad (1)$$

where the subscript pn denotes that this is a potential between a point particle and a nanoparticle, and where  $\mathbf{r}$  is the distance vector between the point particle and the center of the nanoparticle. Because of the spherical symmetry of the density profile and the pair potential  $\phi_{\text{pn}}$ , the effective potential does not depend on the direction of  $\mathbf{r}$ , only on its magnitude  $r = |\mathbf{r}|$ .

Analogously, the effective inter-nanoparticle potential  $V_{\text{nn}}$  for two nanoparticles with internal density profiles  $\rho_1$  and  $\rho_2$ , and corresponding radii  $s_1$  and  $s_2$ , and whose points interact through a pair potential  $\phi_{\text{nn}}$ , is given by

$$V_{\text{nn}}(r) = \int_{\mathcal{B}_{s_1}} d\mathbf{x} \int_{\mathcal{B}_{s_2}} d\mathbf{y} \rho_1(x) \rho_2(y) \phi_{\text{nn}}(|\mathbf{r} - \mathbf{x} - \mathbf{y}|). \quad (2)$$

The potential  $\phi_{\text{nn}}$  will also be assumed to be analytic for  $r > 0$ . Throughout this paper,  $\phi_{\text{pn}}$  and  $\phi_{\text{nn}}$  will be referred to as the *basic pair potentials*, while  $V_{\text{pn}}$  and  $V_{\text{nn}}$  are the *effective potentials*.

To arrive at more concrete expressions for the effective potentials, it will be assumed that the internal density profile of the nanoparticles is analytic, so that it may be written as a Taylor series,

$$\rho(x) = \Theta(s - x) \sum_{\substack{i=0 \\ i \text{ even}}}^{\infty} a_i x^i, \quad (3)$$

where  $\Theta$  is the Heaviside step function. In equation (3), odd powers of  $x$  were omitted since they lead to non-analytic behavior at  $x = 0$ . The potentials for a nanoparticle and a point particle, and for two nanoparticles, respectively, that would result from internal densities of monomial form  $\Theta(s - x)x^i$  are denoted by

$$V_i(r) = \int_{\mathcal{B}_s} d\mathbf{x} x^i \phi_{\text{pn}}(|\mathbf{r} + \mathbf{x}|), \quad (4)$$

$$V_{ij}(r) = \int_{\mathcal{B}_{s_1}} d\mathbf{x} \int_{\mathcal{B}_{s_2}} d\mathbf{y} x^i y^j \phi_{\text{nn}}(|\mathbf{r} + \mathbf{x} - \mathbf{y}|). \quad (5)$$

Here, and below, the dependence of  $V_i$  and  $V_{ij}$  on  $s$  and  $s_1$  and  $s_2$  will not be denoted explicitly. In terms of the potentials  $V_i$  and  $V_{ij}$ , the effective point–nanoparticle and inter-nanoparticle potentials are given by

$$V_{\text{pn}}(r) = \sum_{\substack{i=0 \\ i \text{ even}}}^{\infty} a_i V_i(r) \quad (6)$$

$$V_{\text{nn}}(r) = \sum_{\substack{i=0 \\ i \text{ even}}}^{\infty} \sum_{\substack{j=0 \\ j \text{ even}}}^{\infty} a_i b_j V_{ij}(r) \quad (7)$$

where  $\rho_1(x) = \Theta(s_1 - x) \sum_i a_i x^i$  and  $\rho_2(x) = \Theta(s_2 - x) \sum_j b_j x^j$  are the internal density profiles of two interacting nanoparticles. While often only the first term  $i = j = 0$  will suffice, the formalism will be developed for general  $i$  and  $j$ , since this is not any more difficult.

The three-dimensional and six-dimensional integrals in equations (4) and (5) for the effective potentials make further manipulations cumbersome. However, due to the spherical symmetry of the basic pair potentials, these multidimensional integrals can be rewritten as integrals over a single variable.

To convert equation (4) to a single integral, one goes over to spherical coordinates  $\mathbf{x} = (x \sin \theta \cos \varphi, x \sin \theta \sin \varphi, x \cos \theta)$ , integrates over  $\varphi$  and then performs a change of integration variable from  $\theta$  to  $y = [x^2 \sin^2 \theta + (r - x \cos \theta)^2]^{1/2}$ , which yields

$$V_i(r) = \frac{2\pi}{r} \int_0^s dx \int_{|r-x|}^{r+x} dy x^{i+1} y \phi_{\text{pn}}(y).$$

Reversing the order of the  $x$  and  $y$  integrals and using that  $i$  is even leads to

$$V_i(r) = \frac{2\pi}{(i+2)r} \left[ \int_{|r-s|}^{r+s} dy [s^{i+2} - (r-y)^{i+2}] y \phi_{\text{pn}}(y) + \Theta(s-r) \int_0^{s-r} dy [(r+y)^{i+2} - (r-y)^{i+2}] y \phi_{\text{pn}}(y) \right]. \quad (8)$$

Defining a kernel

$$K_i(x, s) = \frac{2\pi}{i+2} (s^{i+2} - x^{i+2}) \Theta(s - |x|), \quad (9)$$

one can write the right-hand side of equation (8) in the concise form

$$V_i(r) = \frac{1}{r} \int dy K_i(r-y, s) y \phi_{\text{pn}}(|y|), \quad (10)$$

at least for  $r > s$ . That equation (10) also holds for  $r < s$  (with the same expression for  $K_i$ ) is seen by writing the second term in equation (8) as

$$\begin{aligned} & \int_0^{s-r} dy [\{s^{i+2} - (r-y)^{i+2}\} - \{s^{i+2} - (r+y)^{i+2}\}] y \phi_{\text{pn}}(y) \\ &= \int_{-s+r}^{s-r} dy [s^{i+2} - (r-y)^{i+2}] y \phi_{\text{pn}}(|y|). \end{aligned}$$

Combining this with the first term in equation (8) leads again to equation (10). Note that for the special (uniform) case of  $i = 0$ , to be used below, the kernel takes the form

$$K_0(x, s) = \pi(s^2 - x^2) \Theta(s - |x|). \quad (11)$$

For the effective inter-nanoparticle potential  $V_{ij}$ , one can use that the potential energy of two nanoparticles is equivalent to the potential energy of a particle and a nanoparticle of which the points interact via a point-nanoparticle potential  $V_j$ , i.e.,

$$V_{ij}(r) = \frac{1}{r} \int dy K_i(r-y, s_1) y V_j(|y|),$$

where in  $V_j$ , one should replace  $s$  by  $s_2$ , and  $\phi_{\text{pn}}$  by  $\phi_{\text{nn}}$ . Combining this with equation (10), and using that  $K_j(x, s_2)$  is even in  $x$ , one obtains

$$V_{ij}(r) = \frac{1}{r} \int dy dz K_i(r - y, s_1) K_j(y - z, s_2) z \phi_{\text{nn}}(|z|), \quad (12)$$

or

$$V_{ij}(r) = \frac{1}{r} \int dy K_{ij}(r - y, s_1, s_2) y \phi_{\text{nn}}(|y|), \quad (13)$$

with the kernel  $K_{ij}$  given by

$$K_{ij}(x, s_1, s_2) = \int dy K_i(x - y, s_1) K_j(y, s_2). \quad (14)$$

The integral in this expression is further evaluated in the appendix, where it is shown that  $K_{ij}$  is a piecewise polynomial function of degree  $i + j + 5$  which has a finite support  $|x| \leq s_1 + s_2$ , and non-analytic points at  $x = \pm|s_1 - s_2|$ . For the special case  $i = j = 0$  which will be used below, one finds from equations (A.3) and (A.4), and after some rewriting,

$$K_{00}(x, s_1, s_2) = \begin{cases} \frac{\pi^2}{30} (D - |d|)^3 (d^2 + 3D|d| + D^2 - 5x^2) & 0 \text{ if } |x| \leq |d| \\ \frac{\pi^2}{30} (D - |x|)^3 (x^2 + 3D|x| + D^2 - 5d^2) & \text{if } |d| < |x| \leq D \\ 0 & \text{if } |x| > D, \end{cases} \quad (15)$$

where

$$\begin{aligned} D &= s_1 + s_2 \\ d &= s_1 - s_2. \end{aligned} \quad (16)$$

Because the kernels  $K_i$  and  $K_{ij}$  are piecewise polynomials, the integrals in equations (10) and (13) can be performed analytically for many functional forms of  $\phi_{\text{pn}}$  and  $\phi_{\text{nn}}$ , such as power law and exponential forms (see section 5), which are the basis of many commonly used empirical pair potentials.

### 3. Auxiliary potential formulation

When the rigidity assumption is made, some basic potentials allow for overlap, and some do not. Mathematically, the following different overlapping cases can occur: a point particle and a nanoparticle can either overlap (for  $r < s$ ) or not overlap (for  $r > s$ ), while two nanoparticles can have no overlap, which requires  $r > s_1 + s_2 = D$ , or partially overlap, or the smallest nanoparticle can be completely embedded in the larger, which occurs when  $r < |s_1 - s_2| = |d|$ . Although not evident from equations (10) and (13), the non-analytic points of the kernels and of the basic pair potential cause the effective potentials to have different functional forms depending on whether there is overlap. Rather than having to develop separate frameworks for these cases, it is possible to derive one general framework by introducing auxiliary potentials.

Note that even when overlap is not physically allowed, the auxiliary potential formulation is useful, since the effective potentials can be expressed in the auxiliary

potentials, which tend to have a simpler form than the effective potentials themselves. Furthermore, the use of auxiliary potentials will make it straightforward to treat the physical case of hollow particles containing other particles.

The following symmetrization operations on functions  $f$  are useful in denoting the relations between effective and auxiliary potentials<sup>1</sup>:

$$\begin{aligned} f([x]) &= f(x) - f(-x) && \text{'antisymmetrization'} \\ f((x)) &= f(x) + f(-x) && \text{'symmetrization'}. \end{aligned}$$

These operations are also useful for functions with multiple arguments, e.g.,

$$\begin{aligned} f([x], y) &= f(x, y) - f(-x, y) \\ f(x, (y)) &= f(x, y) + f(x, -y) \\ f([x], [y]) &= f(x, y) - f(-x, y) - f(x, -y) + f(-x, -y) \\ f([x, y]) &= f(x, y) - f(-x, -y). \end{aligned}$$

Note that in the last example, a single antisymmetrization was performed which involved both arguments.

The expressions of the effective potentials  $V_i$  and  $V_{ij}$  in terms of auxiliary potentials (whose derivations will follow) are given by

$$V_i(r) = \begin{cases} A_i((r), s) & \text{if } r < s \\ A_i(r, [s]) & \text{if } r > s \end{cases} \quad (17)$$

$$V_{ij}(r) = \begin{cases} A_{ij}((r), [s_1], s_2) & \text{if } r < |d| \text{ and } s_1 < s_2 \\ A_{ij}((r), s_1, [s_2]) & \text{if } r < d \text{ and } s_1 > s_2 \\ A_{ij}((r), s_1, s_2) - A_{ij}(r, (s_1, -s_2)) & \text{if } |d| < r < D \\ A_{ij}(r, [s_1], [s_2]) & \text{if } r > D, \end{cases} \quad (18)$$

where the auxiliary potentials are defined as

$$A_i(r, s) = \frac{1}{r} \int_0^{r+s} dy \bar{K}_i(r-y, s) y \phi_{\text{pn}}(y) \quad (19)$$

$$A_{ij}(r, s_1, s_2) = \frac{1}{r} \int_0^{r+s_1+s_2} dy \bar{K}_{ij}(r-y, s_1, s_2) y \phi_{\text{nm}}(y), \quad (20)$$

in which furthermore

$$\bar{K}_i(x, s) = \frac{2\pi}{i+2} (s^{i+2} - x^{i+2}) \quad (21)$$

$$\bar{K}_{ij}(x, s_1, s_2) = \int_{-s_2}^{x+s_1} dy \bar{K}_i(x-y, s_1) \bar{K}_j(y, s_2). \quad (22)$$

Note that  $\bar{K}_i$  is the analytic continuation of  $K_i$ , while the quantity  $\bar{K}_{ij}(x, s_1, s_2)$  has the same functional form as the kernel  $K_{ij}$  for  $x < 0$ ,  $d < |x| < D$  (as it coincides with *case 4* in the appendix). In particular, for  $i = j = 0$ , one has from equation (15)

$$\bar{K}_{00}(x, s_1, s_2) = \frac{\pi^2}{30} (s_1 + s_2 + x)^3 (x^2 - 3s_1x - 3s_2x - 4s_1^2 - 4s_2^2 + 12s_1s_2). \quad (23)$$

<sup>1</sup> This notation is similar to the so-called Bach brackets used to denote symmetrized and antisymmetrized tensors in general relativity; see e.g. [26].

### 3.1. Effective potential between a point particle and a nanoparticle

The derivation of equation (17) goes as follows. Consider first the non-overlapping case  $r > s$ . In that case, the absolute value sign in the argument of  $\phi_{\text{pn}}$  may be dropped in equation (10), since  $r > s$  and  $r - y < s$  (cf equation (9)) imply that  $y > 0$ . Thus, the effective point–nanoparticle potential can be written as

$$\begin{aligned} V_i(r) &= \frac{1}{r} \int dy K_i(r - y, s) y \phi_{\text{pn}}(y) = \frac{1}{r} \int_{r-s}^{r+s} dy \bar{K}_i(r - y, s) y \phi_{\text{pn}}(y) \\ &= \frac{1}{r} \int_0^{r+s} dy \bar{K}_i(r - y, s) y \phi_{\text{pn}}(y) + \frac{1}{r} \int_{r-s}^0 dy \bar{K}_i(r - y, s) y \phi_{\text{pn}}(y) \\ &= A_i(r, s) - A_i(r, -s) = A_i(r, [s]). \end{aligned} \quad (24)$$

For the case  $r < s$ , the argument in the  $\phi_{\text{pn}}$  function in equation (10) needs to be  $-y$  for  $y < 0$ , giving

$$\begin{aligned} V_i(r) &= \frac{1}{r} \int_0^{r+s} dy \bar{K}_i(r - y, s) y \phi_{\text{pn}}(y) + \frac{1}{r} \int_{r-s}^0 dy \bar{K}_i(r - y, s) y \phi_{\text{pn}}(-y) \\ &= \frac{1}{r} \int_0^{r+s} dy \bar{K}_i(r - y, s) y \phi_{\text{pn}}(y) - \frac{1}{r} \int_0^{s-r} dy \bar{K}_i(-r - y, s) y \phi_{\text{pn}}(y), \end{aligned} \quad (25)$$

where a change of integration variable from  $y$  to  $-y$  was carried out in the second integral, and it was used that  $\bar{K}_i(y, s)$  is even in  $y$ . The first term on the right-hand side of equation (25) is equal to  $A_i(r, s)$  in equation (19), while the second term equals  $A_i(-r, s)$ , so

$$V_i(r) = A_i(r, s) + A_i(-r, s) \equiv A_i((r), s). \quad (26)$$

Thus, although the effective potentials between a point particle and a nanoparticle have different forms for non-overlapping and overlapping situations (equations (24) and (26), respectively), both can be written in terms of the auxiliary potential  $A_i$ , and one obtains equation (17).

A technical difficulty must be mentioned here, namely, that the integral defining the auxiliary potential in equation (19) may not converge, even when the linear combinations in equation (17) do. In such cases, one should strictly write the auxiliary potential as a sum of a regular and a diverging part by replacing the lower limit of the integral in equation (19) by  $\delta > 0$ , and expanding the result in  $\delta$ . In the absence of overlap, equation (17) must yield a finite result, i.e., the diverging parts (negative powers of  $\delta$  and possibly logarithmic terms) must cancel; hence in that case it suffices to work with the regular part of the auxiliary potential. On the other hand, in the case of overlap, it is possible that the divergent parts do not cancel in equation (26), resulting in infinite effective potentials. An independent criterion for whether an effective potential is infinite in overlapping cases can be constructed as follows. For a single particle inside a nanoparticle, the effective potential becomes infinite only if the divergence of the basic pair potential  $\phi_{\text{pn}}$  at the origin is too strong. In particular, if  $\phi(r) \propto r^{-k}$  for small  $r$  then the point–nanoparticle potential is infinite for  $k \geq 3$ , as is seen by considering a small sphere around the particle, giving an integral of the form  $\int_{r<\delta} d\mathbf{r} \phi(r) \propto \int_0^\delta dr r^2 r^{-k} \sim (\delta^{3-k}/(3-k))$ , which diverges for  $k \geq 3$  in the limit  $\delta \rightarrow 0$ . This result extends to inter-nanoparticle potentials, which

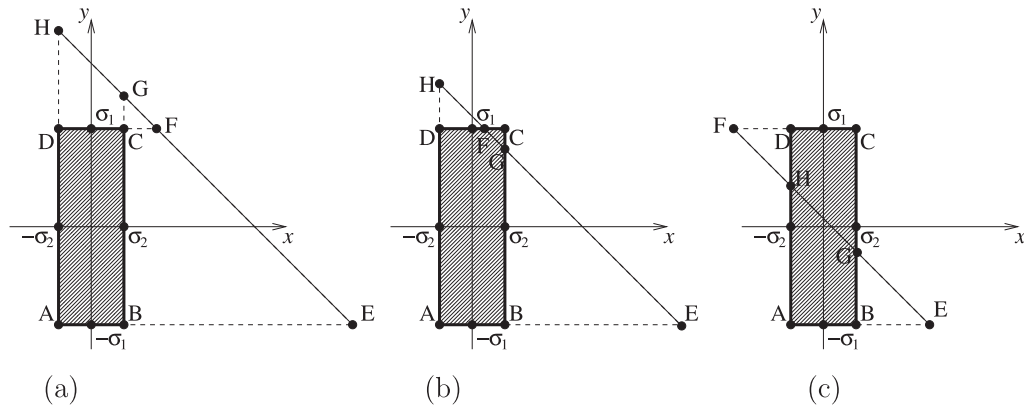


**Figure 2.** Subdivision of the integration domain in the derivation of the expression of the inter-nanoparticle effective potential  $V_{ij}$  in terms of the auxiliary potential  $A_{ij}$ . Assuming  $s_1 > s_2$ , three cases have been distinguished: (a)  $r > s_1 + s_2$ , (b)  $s_1 - s_2 < r < s_1 + s_2$ , and (c)  $r < s_1 - s_2$ .

are also infinite if there is overlap and the potential  $\phi_{\text{nn}}$  diverges no slower than  $r^{-3}$ , i.e., the  $V_{ij}(r)$  are finite for  $r < D$  provided  $\phi_{\text{nn}}(r)$  diverges for small  $r$  slower than  $r^{-3}$ . Given this criterion, the divergent part of an auxiliary potential is not needed to determine whether the corresponding effective potential is infinite. Since the divergent parts are needed neither in overlapping nor in non-overlapping cases, below, only the regular parts of auxiliary potentials will be given.

### 3.2. Effective potential between two nanoparticles

To derive equation (18) for the effective potentials between two nanoparticles, one starts by rewriting equation (12) as

$$V_{ij}(r) = \frac{1}{r} \int_{-s_1}^{s_1} dy \int_{-s_2}^{s_2} dx \bar{K}_i(y, s_1) \bar{K}_j(x, s_2) (r - x - y) \phi_{\text{nn}}(|r - x - y|). \quad (27)$$

In this formulation, the integration domain is a rectangle in the  $(x, y)$  plane and the integrand has a diagonal non-analytic line at  $x + y = r$ . This diagonal line may or may not cross the domain, which is what gives rise to non-analyticity and the difference between overlapping and non-overlapping effective potentials.

Subdividing the domain into triangular regions without non-analyticities will result in expressions in terms of analytic subexpressions. The appropriate subdivisions of the integration domain are shown in figure 2, where it was assumed that the radius  $s_1$  is larger than the radius  $s_2$ . The three panels of the figure correspond to the three cases that need to be distinguished: (a) no overlap:  $r > s_1 + s_2$ , (b) partial overlap:  $s_1 - s_2 < r < s_1 + s_2$ , and (c) complete overlap,  $r < s_1 - s_2$ . In all three panels of figure 2, the rectangle ABCD is the integration domain, and the diagonal line through points E and H is the line of non-analyticities (where  $r - x - y = 0$ ). For points below this line, the absolute value in the argument of  $\phi_{\text{nn}}$  in equation (27) may be omitted, while for points above this line, it changes the sign of the argument. Considering first case (a), i.e., no overlap, one sees

from figure 2(a) that

$$V_{ij}(r) = I_{\text{AEH}}^+ - I_{\text{BEG}}^+ - I_{\text{DFH}}^+ + I_{\text{CFG}}^+, \quad (28)$$

where  $I_{\text{XYZ}}^+$  is the integral (27) with the absolute value sign omitted, and evaluated over the area of the triangle XYZ. For case (b), i.e., partial overlap, one finds from figure 2(b)

$$V_{ij}(r) = I_{\text{AEH}}^+ - I_{\text{BEG}}^+ - I_{\text{DFH}}^+ + I_{\text{CFG}}^-, \quad (29)$$

where the superscript ‘-’ indicates that the sign of the argument of  $\phi_{\text{nn}}$  in equation (27) is changed. Finally for case (c), one finds from figure 2(c)

$$V_{ij}(r) = I_{\text{AEH}}^+ - I_{\text{BEG}}^+ - I_{\text{DFH}}^- + I_{\text{CFG}}^-. \quad (30)$$

Note that for even basic potentials  $\phi_{\text{pn}}$  and  $\phi_{\text{nn}}$ , the sign of the arguments is inconsequential, so all three cases (28)–(30) will have the same functional form.

The integration limits appropriate for the triangular regions are easily determined from figure 2, yielding the following explicit expression for the integral  $I_{\text{AEH}}^+$ :

$$\begin{aligned} I_{\text{AEH}}^+ &= \frac{1}{r} \int_{-s_2}^{r+s_1} dx \int_{-s_1}^{r-x} dy \bar{K}_i(y, s_1) \bar{K}_j(x, s_2) (r-x-y) \phi_{\text{nn}}(r-x-y) \\ &= A_{ij}(r, s_1, s_2). \end{aligned} \quad (31)$$

Here, the identification with  $A_{ij}$  followed from equations (20) and (22). Given the form of the auxiliary potential in equation (31), it is not hard to show that

$$\begin{aligned} I_{\text{BEG}}^+ &= A_{ij}(r, s_1, -s_2), \\ I_{\text{DFH}}^+ &= A_{ij}(r, -s_1, s_2), \\ I_{\text{CFG}}^+ &= A_{ij}(r, -s_1, -s_2), \end{aligned} \quad (32)$$

so with equation (28) one finds for the non-overlapping case

$$\begin{aligned} V_{ij}(r) &= A_{ij}(r, s_1, s_2) - A_{ij}(r, s_1, -s_2) - A_{ij}(r, -s_1, s_2) + A_{ij}(r, -s_1, -s_2) \\ &= A_{ij}(r, [s_1], [s_2]). \end{aligned} \quad (33)$$

As was the case for  $A_i$ ,  $A_{ij}$  may have divergent parts which cancel in equation (33) and will be omitted below.

According to equations (28) and (29), the partially overlapping case (b) only requires replacing  $I_{\text{CFG}}^+$  by  $I_{\text{CFG}}^-$ , which is given by

$$I_{\text{CFG}}^- = \frac{1}{r} \int_{r-s_1}^{s_2} dx \int_{r-x}^{s_1} dy \bar{K}_i(y, s_1) \bar{K}_j(x, s_2) (r-x-y) \phi_{\text{nn}}(-r+x+y). \quad (34)$$

Making the substitutions  $y \rightarrow -y$ ,  $x \rightarrow -x$ , and using that  $\bar{K}_i$  and  $\bar{K}_j$  are even in  $x$  and  $y$ , one finds

$$I_{\text{CFG}}^- = A_{ij}(-r, s_1, s_2), \quad (35)$$

so for  $d < r < D$

$$\begin{aligned} V_{ij}(r) &= A_{ij}(r, s_1, s_2) - A_{ij}(r, s_1, -s_2) - A_{ij}(r, -s_1, s_2) + A_{ij}(-r, s_1, s_2) \\ &= A_{ij}(r, s_1, s_2) - A_{ij}(r, (s_1, -s_2)). \end{aligned} \quad (36)$$

For the fully overlapping case, finally, one furthermore needs to replace  $I_{\text{DFH}}^+$  by

$$I_{\text{DFH}}^- = \frac{1}{r} \int_{r-s_1}^{-s_2} dx \int_{r-z}^{s_1} dy \bar{K}_i(y, s_1) \bar{K}_j(x, s_2) (r-x-y) \phi_{\text{nn}}(-r+x+y) = A_{ij}(-r, s_1, -s_2), \quad (37)$$

whence for  $r < d$

$$V_{ij}(r) = A_{ij}(r, s_1, s_2) - A_{ij}(r, s_1, -s_2) - A_{ij}(-r, s_1, -s_2) + A_{ij}(-r, s_1, s_2) = A_{ij}((r), s_1, [s_2]). \quad (38)$$

The reason that this is not symmetric in  $s_1$  and  $s_2$  is because of the assumption that  $s_1 > s_2$ . With  $s_1 < s_2$  and  $r < s_2 - s_1$ , one would have obtained  $V_{ij}(r) = A_{ij}((r), [s_1], s_2)$ . This completes the derivation of equation (18).

### 3.3. Ambiguity in the auxiliary potentials

There is a degree of freedom in choosing the auxiliary potentials in equations (17) and (18), since they enter only in specific combinations. In particular, according to equation (17), the effective point–nanoparticle potential is either  $r$  symmetric or  $s$  antisymmetric. Thus, one may replace  $A_i(r, s)$  by  $A_i(r, s) + X(r, s)$  if the function  $X(r, s)$  is antisymmetric in  $r$  as well as symmetric in  $s$ , i.e., if

$$X(r, s) = X(r, -s) = -X(-r, s). \quad (39)$$

Conversely, any terms in  $A_i$  that satisfy equation (39) are irrelevant to equation (17) and may, therefore, be omitted. Similarly, the effective inter-nanoparticle potential in equation (18) is not affected by adding a function  $Y(r, s_1, s_2)$  to the auxiliary potential  $A_{ij}$ , as long as  $Y$  satisfies

$$\begin{aligned} Y(r, s_1, s_2) - Y(r, -s_1, s_2) - Y(r, s_1, -s_2) + Y(r, -s_1, -s_2) &= 0 \\ Y(r, s_1, s_2) &= Y(-r, -s_1, -s_2), \end{aligned} \quad (40)$$

while terms present in  $A_{ij}$  that satisfy these relations are irrelevant, and may be omitted.

## 4. Solid and hollow nanoparticles

Two particular cases of the internal nanoparticle densities  $\rho$  will be considered in detail below. The first is the case of a uniform internal density  $\rho$  inside a solid sphere of radius  $s$ :

$$\rho(x) = \rho\Theta(s-x). \quad (41)$$

Since equation (41) is of the form  $a_i\Theta(s-x)x^i$  with  $i = 0$  and  $a_0 = \rho$ , equation (6) gives for the effective point–nanoparticle potential

$$V_{\text{pn}}(r) = \rho V_0(r). \quad (42)$$

Similarly, the effective inter-nanoparticle potential of two solid nanoparticles of uniform density  $\rho_1$  and  $\rho_2$ , and radii  $s_1$  and  $s_2$ , respectively, satisfies (cf equation (7))

$$V_{\text{nn}}(r) = \rho_1\rho_2 V_{00}(r). \quad (43)$$

The second type of ‘internal’ density  $\rho(x)$  considered here is that of hollow nanoparticles, whose density is concentrated on the surface of the sphere, i.e.,

$$\rho(x) = \tilde{\rho} \delta(s - x), \quad (44)$$

where  $\tilde{\rho}$  is the surface density on the area of the sphere of size  $s$ . This density is appropriate for describing e.g. buckyballs [21]. This density could be seen as the limit of a spherical shell with a thickness  $h$  which is taken to go to zero. One may therefore obtain the effective potentials for this case by subtracting two effective potentials, as was done for instance in [1] and [17]. Starting from equation (44), however, the limiting process is not needed. The density in equation (44) cannot be written in the form of equation (3), but it is linked to the uniform internal density in equation (41) by

$$\tilde{\rho} \delta(s - x) = \tilde{\rho} \frac{\partial \Theta(s - x)}{\partial s}. \quad (45)$$

Consequently, the effective point–nanoparticle potential for this case is given by

$$V_{\text{pn}}(r) = \tilde{\rho} V_{\text{h}}(r), \quad (46)$$

with

$$V_{\text{h}}(r) = \frac{\partial V_0(r)}{\partial s}, \quad (47)$$

where the subscript h indicates that this potential acts between a hollow nanoparticle and a point particle.

In a similar fashion, the inter-nanoparticle potentials for a solid and a hollow nanoparticle (sh) is given by

$$V_{\text{nn}}(r) = \rho_1 \tilde{\rho}_2 V_{\text{sh}}(r) \quad (48)$$

and the potential for two hollow nanoparticles (hh) satisfies

$$V_{\text{nn}}(r) = \tilde{\rho}_1 \tilde{\rho}_2 V_{\text{hh}}(r), \quad (49)$$

where  $\tilde{\rho}_1$  and  $\tilde{\rho}_2$  are the surface density of the two nanoparticles, while the scaled inter-nanoparticle potentials in equations (48) and (49) are given by

$$\begin{aligned} V_{\text{sh}}(r) &= \frac{\partial V_{00}(r)}{\partial s_2} \\ V_{\text{hh}}(r) &= \frac{\partial^2 V_{00}(r)}{\partial s_1 \partial s_2}. \end{aligned} \quad (50)$$

Thus, the effective potentials  $V_{\text{h}}$ ,  $V_{\text{sh}}$  and  $V_{\text{hh}}$  can be found by differentiation once  $V_0$  and  $V_{00}$ , are known.

The effective potentials for solid nanoparticles can be expressed in terms of auxiliary potentials  $A_0$  and  $A_{00}$  using equations (17) and (18). In applying equations (47) and (50) to these expressions, it should be realized that taking a derivative turns an

antisymmetrized function into a symmetrized one, and vice versa. Thus, by defining

$$\begin{aligned} A_h(r, s) &= \frac{\partial A_0(r, s)}{\partial s} \\ A_{sh}(r, s_1, s_2) &= \frac{\partial A_{00}(r, s_1, s_2)}{\partial s_2} \\ A_{hh}(r, s_1, s_2) &= \frac{\partial^2 A_{00}(r, s_1, s_2)}{\partial s_1 \partial s_2}, \end{aligned} \quad (51)$$

one gets for the effective potentials

$$V_h(r) = \begin{cases} A_h(r, s) & \text{if } r < s \\ A_h(r, s) & \text{if } r > s, \end{cases} \quad (52)$$

$$V_{sh}(r) = \begin{cases} A_{sh}(r, [s_1], s_2) & \text{if } r < |d| \text{ and } s_1 < s_2 \\ A_{sh}(r, s_1, (s_2)) & \text{if } r < d \text{ and } s_1 > s_2 \\ A_{sh}(r, s_1, s_2) + A_{sh}(r, [s_1], -s_2) & \text{if } |d| < r < D \\ A_{sh}(r, [s_1], (s_2)) & \text{if } r > D, \end{cases} \quad (53)$$

$$V_{hh}(r) = \begin{cases} A_{hh}(r, (s_1), s_2) & \text{if } r < |d| \text{ and } s_1 < s_2 \\ A_{hh}(r, s_1, (s_2)) & \text{if } r < d \text{ and } s_1 > s_2 \\ A_{hh}(r, s_1, s_2) + A_{hh}(r, (s_1), -s_2) & \text{if } |d| < r < D \\ A_{hh}(r, (s_1), (s_2)) & \text{if } r > D. \end{cases} \quad (54)$$

## 5. Effective potentials for uniformly solid and hollow nanoparticles

### 5.1. Power laws

Pair potentials of power law form

$$\phi^n(r) = \frac{1}{r^n}, \quad (55)$$

with  $n$  integer, are basic building blocks of many atomic and molecular pair potentials, such as the Coulomb potential ( $n = 1$ ) and the Lennard-Jones potential (a linear combination of  $n = 6$  and  $12$ ). Note that here and below, a superscript on a potential represents an index, not a power.

The effective potential  $V_0^n$  for a point particle and a solid nanoparticle of radius  $s$  whose points interact with the particle through  $\phi_{pn} = \phi^n$  is given in terms of the auxiliary potential by equation (17). The auxiliary potential follows from equations (19), giving, for general  $n$ ,

$$\begin{aligned} A_0^n(r, s) &= \frac{\pi}{r} \int_0^{r+s} dy \frac{s^2 - (r-y)^2}{y^{n-1}} \\ &= \frac{2\pi[r + (n-3)s]}{(n-2)(n-3)(n-4)r(r+s)^{n-3}}, \end{aligned} \quad (56)$$

where divergent terms were omitted, as explained in section 3.1.

The right-hand side of equation (56) becomes ill-defined for the specific values  $n = 2, 3$  and  $4$ . This problem is caused by a term proportional to  $x^{n'-n-1}$  in the integrand in equation (56) (with  $n' = 2, 3$  or  $4$ ), which when  $n = n'$  should have resulted in a term  $\ln(r+s)$  instead of the erroneous and ill-defined expression  $((r+s)^{n'-n}/(n'-n))$  that occurs in equation (56). Using that  $\lim_{n \rightarrow n'} (\partial/\partial n)[(n-n')(x^{n'-n}/(n'-n))] = \ln x$ , this can be fixed by making the substitution

$$A^{n'} \longrightarrow \lim_{n \rightarrow n'} \frac{\partial}{\partial n} [(n-n')A^n]. \quad (57)$$

Applied to equation (56), this gives

$$\begin{aligned} A_0^2(r, s) &= \frac{\pi(r+s)(3r-s)}{2r} + \frac{\pi(s^2-r^2)}{r} \ln(r+s) \\ A_0^3(r, s) &= -\frac{2\pi s}{r} + 2\pi \ln(r+s) \\ A_0^4(r, s) &= -\frac{\pi(3r+s)}{2r(r+s)} - \frac{\pi}{r} \ln(r+s). \end{aligned} \quad (58)$$

The effective potential  $V_0^n$  is obtained from these expressions for the auxiliary potential using equation (17).

From equations (51) and (56), it follows that the auxiliary potential for a hollow nanoparticle and a point particle is given by

$$A_h^n(r, s) = -\frac{2\pi s}{(n-2)r(r+s)^{n-2}}. \quad (59)$$

Equation (59) is ill-defined for  $n = 2$ , in which case one uses equation (57) to find

$$A_h^2(r, s) = \frac{2\pi s}{r} \ln(r+s). \quad (60)$$

The effective potential  $V_h^n$  is now obtained from equation (52).

For the effective inter-nanoparticle potential  $V_{00}$ , the auxiliary potential formulation (18) holds with  $i = j = 0$ , where the auxiliary potential is found using equation (20) with  $\phi_{nn} = \phi^n$ , giving

$$A_{00}^n(r, s_1, s_2) = \frac{4\pi^2 p_n(r, s_1, s_2)}{(n-7)(n-6)(n-5)(n-4)(n-3)(n-2)r(r+s_1+s_2)^{n-5}}, \quad (61)$$

where

$$p_n(r, s_1, s_2) = r^2 + (n-5)(s_1+s_2)r + (n-6)[s_1^2 + s_2^2 + (n-5)s_1s_2]. \quad (62)$$

The expression in equation (61) is ill-defined for  $n = 2, 3, 4, 5, 6$  and  $7$ . Using again equation (57), the correct expression for  $A_{00}^n$  for these values of  $n$  is found to be

$$\begin{aligned} A_{00}^n(r, s_1, s_2) &= \frac{4\pi^2}{r(r+s_1+s_2)^{n-5} \prod_{\substack{\ell=2 \\ \ell \neq n}}^7 (\ell-n)} \\ &\times \left\{ p_n(r, s_1, s_2) \left[ \ln(r+s_1+s_2) - \sum_{\substack{\ell=2 \\ \ell \neq n}}^7 \frac{1}{\ell-n} \right] \right. \\ &\left. - s_1^2 - s_2^2 - (s_1+s_2)r + (11-2n)s_1s_2 \right\}. \end{aligned} \quad (63)$$

According to equation (51), the auxiliary potential for a solid sphere of radius  $s_1$  and a hollow sphere of radius  $s_2$  can be found by taking the derivative with respect to  $s_2$ , yielding, for general  $n$ ,

$$A_{\text{sh}}^n(r, s_1, s_2) = \frac{-4\pi^2 s_2 [r + (n-4)s_1 + s_2]}{(n-5)(n-4)(n-3)(n-2)r(r+s_1+s_2)^{n-4}}. \quad (64)$$

Finally, the effective potential for two hollow spheres follows from another derivative with respect to  $s_1$  (cf equation (51)), leading to

$$A_{\text{hh}}^n(r, s_1, s_2) = \frac{4\pi^2 s_1 s_2}{(n-3)(n-2)r(r+s_1+s_2)^{n-3}}. \quad (65)$$

For the ill-defined cases of equations (64) and (65), one can use equation (57) to get expressions similar to the one in equation (63).

## 5.2. Exponentials

The effective interactions as a result of the exponential pair potential

$$\phi^{\text{E}}(r) = e^{-r} \quad (66)$$

will now be derived. Substituting this potential for  $\phi_{\text{pn}}$  in the expression (19) for the auxiliary potential gives

$$A_0^{\text{E}}(r, s) = \frac{2\pi(3+r+sr+s^2+3s)}{r} e^{-r-s} + 4\pi, \quad (67)$$

where an irrelevant expression satisfying equation (39) was omitted. From equations (51) and (67), the auxiliary potential for a point particle and a hollow nanoparticle is found to be

$$A_{\text{h}}^{\text{E}}(r) = -\frac{2\pi s(1+r+s)}{r} e^{-r-s}. \quad (68)$$

Note that the corresponding effective potentials follow from equations (17) and (52).

The effective inter-nanoparticle potential is of the auxiliary potential form (18) with  $i = j = 0$ . The auxiliary potential  $A_{00}^{\text{E}}$  is found using equation (20) with  $\phi_{\text{nn}} = \phi^{\text{E}}$ , giving

$$\begin{aligned} A_{00}^{\text{E}}(r, s_1, s_2) &= 4\pi^2 \frac{(r+s_1+s_2+5)(s_1+1)(s_2+1)+1-s_1s_2}{r} e^{-r-s_1-s_2} \\ &+ \frac{\pi^2}{3r} [8(s_1+s_2)(s_1^2+s_2^2-s_1s_2)r+6(s_1^2+s_2^2-4)(r^2+4) \\ &-r^4+3(s_1^2-s_2^2)^2+24], \end{aligned} \quad (69)$$

where an expression satisfying equation (40) has been omitted. Using equations (51), the auxiliary potentials for the interactions between a solid and a hollow nanoparticle and between two hollow particles are found to be

$$\begin{aligned} A_{\text{sh}}^{\text{E}}(r, s_1, s_2) &= \frac{-4\pi^2 s_2 [(r+s_1+s_2+4)(s_1+1)-s_1]}{r} e^{-r-s_1-s_2} \\ &+ \frac{4\pi^2 s_2 [(r+s_2)^2-s_1^2+4]}{r} \end{aligned} \quad (70)$$

$$A_{\text{hh}}^{\text{E}}(r, s_1, s_2) = \frac{4\pi^2 s_1 s_2 (r+s_1+s_2+2)}{r} e^{-r-s_1-s_2} - \frac{8\pi^2 s_1 s_2}{r}. \quad (71)$$

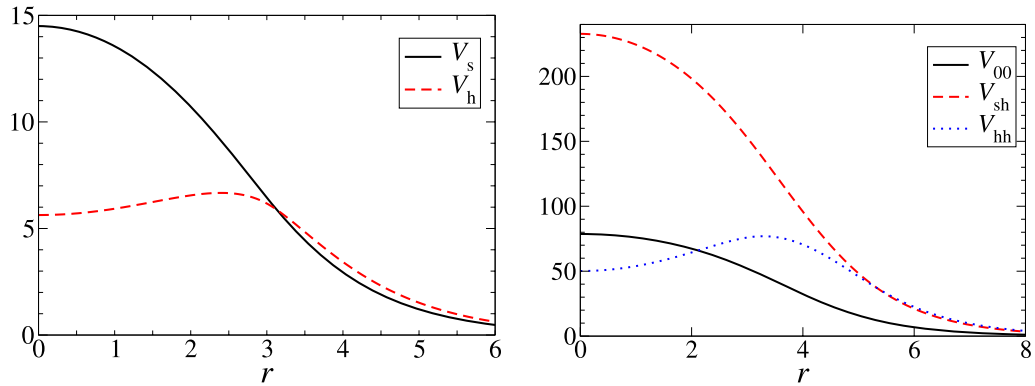


**Figure 3.** Typical example of effective potentials based on an exponential interaction (equations (18) and (69)). The left panel shows the point–nanoparticle potentials for solid (s) and hollow (h) spheres with radius  $s = 3$ , while the right panel shows the inter–nanoparticle potentials for radii  $s_1 = 4$  and  $s_2 = 1$ .

Figure 3 shows a typical example of the effective potentials derived from the exponential basic potential (cf equations (17), (18), (52)–(54) and (67)–(71)). One sees that these effective potentials are very smooth and do not have a hard core, which is typical for effective potentials based on a basic pair potential that does not diverge for small distances.

### 5.3. Examples using common pair potentials

*London–van der Waals potential.* In this section, the effective potentials based on the London–van der Waals potential

$$\phi^6(r) = \frac{1}{r^6} \quad (72)$$

will be presented. Note that the negative prefactor that occurs in front of the attractive London–van der Waals interaction has been omitted here. Substituting  $n = 6$  into equation (56), and using equation (17), one finds the London–van der Waals potential for a solid nanoparticle and a point particle:

$$V_0^6(r) = \frac{4\pi s^3}{3(r^2 - s^2)^3}, \quad (73)$$

for  $r > s$ . This effective potential becomes infinite for  $r < s$ . For the London–van der Waals interaction of a hollow nanoparticle with a point particle, equations (52) and (59), with  $n = 6$ , lead to

$$V_h^6(r) = \frac{4\pi s^2}{(r^2 - s^2)^3} + \frac{8\pi s^4}{(r^2 - s^2)^4}. \quad (74)$$

The effective London–van der Waals interaction potential for two solid nanoparticles is determined by substituting  $n = 6$  into equation (63), and using equation (18), which

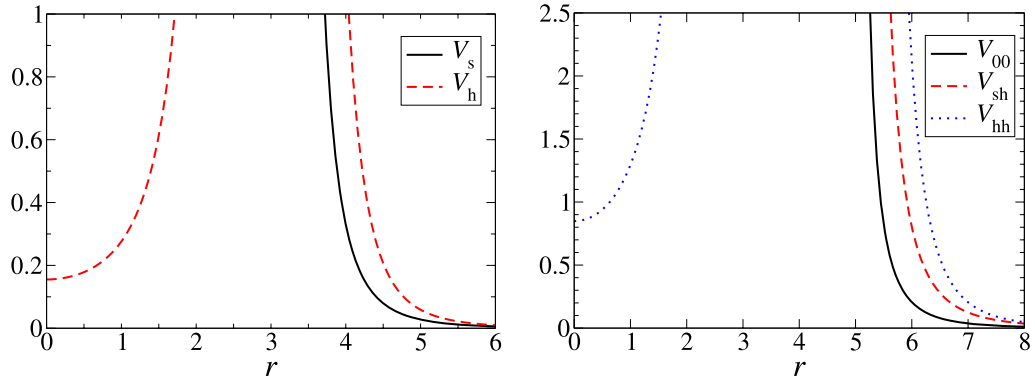


**Figure 4.** Typical example of effective potentials based on the London–van der Waals interaction, i.e., the power law in equation (55) with  $n = 6$ . The left panel shows the potential for a point particle and solid or hollow nanoparticle of radius  $s = 3$ ; the right panel shows the potential for two nanoparticles of radius  $s_1 = 4$  and  $s_2 = 1$ .

gives

$$V_{00}^6(r) = \frac{\pi^2 s_1 s_2}{3(r^2 - d^2)} + \frac{\pi^2 s_1 s_2}{3(r^2 - D^2)} + \frac{\pi^2}{6} \ln \frac{r^2 - D^2}{r^2 - d^2}. \quad (75)$$

This result coincides with that of Hamaker [20].

Using equations (50) and (75), or using equations (64) and (53), one finds for the London–van der Waals potential  $V_{sh}^6$  for a solid nanoparticle of radius  $s_1$  and a hollow nanoparticle of radius  $s_2$

$$V_{sh}^6(r) = \frac{2\pi^2 s_1 s_2 D}{3(r^2 - D^2)^2} - \frac{2\pi^2 s_1 s_2 d}{3(r^2 - d^2)^2} - \frac{\pi^2 s_2}{3(r^2 - D^2)} + \frac{\pi^2 s_2}{3(r^2 - d^2)}. \quad (76)$$

The effective London–van der Waals potential  $V_{hh}^6$  for two hollow nanoparticles, finally, is obtained from equation (76) using equation (50), or alternatively from equations (65) and (54), with the result

$$V_{hh}^6(r) = \frac{8\pi^2 s_1 s_2 D^2}{3(r^2 - D^2)^3} - \frac{8\pi^2 s_1 s_2 d^2}{3(r^2 - d^2)^3} + \frac{2\pi^2 s_1 s_2}{3(r^2 - D^2)^2} - \frac{2\pi^2 s_1 s_2}{3(r^2 - d^2)^2}. \quad (77)$$

Figure 4 shows a typical example of the effective potentials for the London–van der Waals interaction as the basic pair potential.

*Morse potential.* The Morse potential [29]

$$\phi^M(r) = e^{-2b(r-1)} - 2e^{-b(r-1)}, \quad (78)$$

is used e.g. for molecular bonds and for pure metals [30]. It is a sum of two exponential functions, so having derived the formulae for the exponential potential in section 5.2, one

Effective pair potentials for spherical nanoparticles

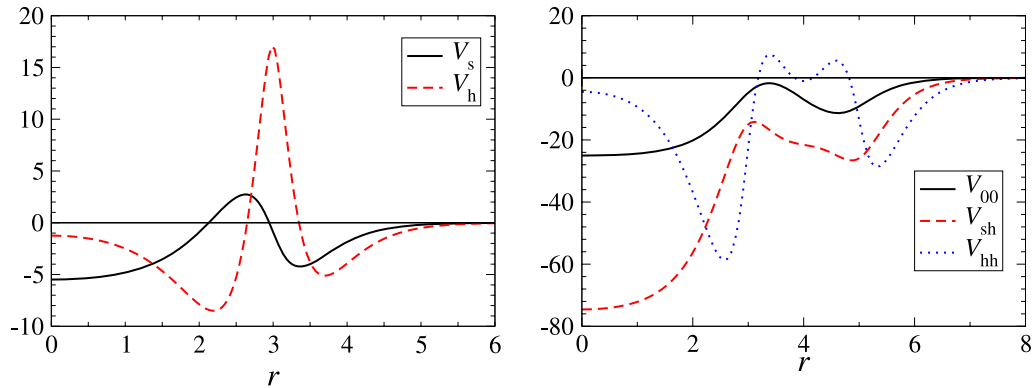


**Figure 5.** Example of Morse effective potentials for  $b = 2.6$ . The left panel shows the effective potential for a particle and a solid or hollow nanoparticle of radius  $s = 3$ ; the right panel shows the effective potentials for two nanoparticles of radius  $s_1 = 4$  and  $s_2 = 1$ .

easily finds the corresponding point–nanoparticle interactions by taking the combinations

$$V_0^M(r) = \frac{e^{2b}}{2^3 b^3} V_0^E(2br, 2bs) - \frac{2e^b}{b^3} V_0^E(br, bs) \tag{79}$$

$$V_h^M(r) = \frac{e^{2b}}{2^2 b^2} V_h^E(2br, 2bs) - \frac{2e^b}{b^2} V_h^E(br, bs), \tag{80}$$

where the notation  $V_0^E(\alpha r, \beta s)$  indicates that in  $V_0^E$  and  $V_h^E$ ,  $r$  is to be replaced by  $\alpha r$  and  $s$  by  $\beta s$ . Likewise, the inter-nanoparticle interactions for the Morse potential in equation (78) are given by

$$V_{00}^M(r) = \frac{e^{2b}}{2^6 b^6} V_{00}^E(2br, 2bs_1, 2bs_2) - \frac{2e^b}{b^6} V_{00}^E(br, bs_1, bs_2). \tag{81}$$

$$V_{sh}^M(r) = \frac{e^{2b}}{2^5 b^5} V_{sh}^E(2br, 2bs_1, 2bs_2) - \frac{2e^b}{b^5} V_{sh}^E(br, bs_1, bs_2). \tag{82}$$

$$V_{hh}^M(r) = \frac{e^{2b}}{2^4 b^4} V_{hh}^E(2br, 2bs_1, 2bs_2) - \frac{2e^b}{b^4} V_{hh}^E(br, bs_1, bs_2). \tag{83}$$

Two examples of the Morse-based effective potentials are shown in figures 5 and 6, for  $b = 2.6$  and  $b = 5.6$ , respectively. For the lower value of  $b$ , there is a low barrier to a point particle penetrating a nanoparticle as well as to one nanoparticle penetrating another (cf figure 5), while for the larger value of  $b$  this is virtually impossible (cf figure 6) if the energies of the particles are of order 1.

*Buckingham potential.* The modified Buckingham potential [31]

$$\phi^B(r) = \begin{cases} \infty & \text{if } r < r^*, \\ ae^{-br} - cr^{-6} & \text{if } r > r^*, \end{cases} \tag{84}$$

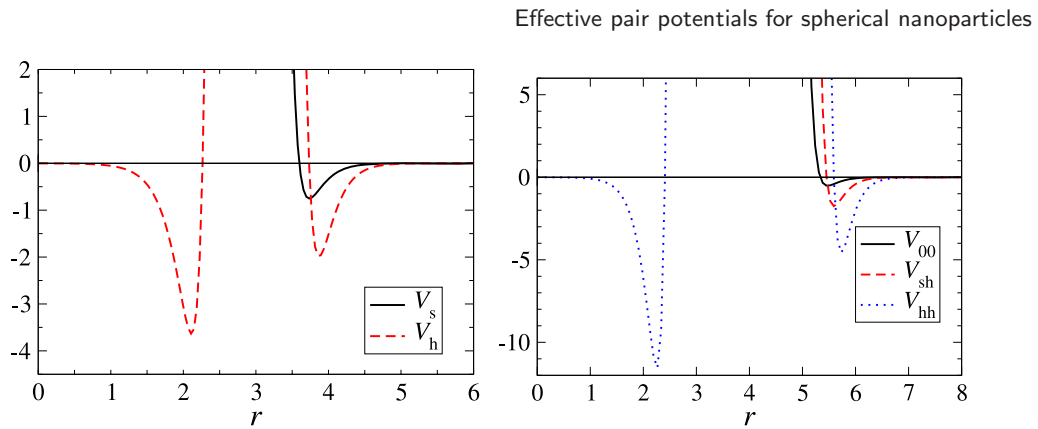


**Figure 6.** Example of Morse effective potentials for  $b = 5.6$ , for which the Morse potential resembles the Lennard-Jones potential. The left panel shows the effective point–nanoparticle potentials for  $s = 3$ ; the right panel shows the effective potentials for two nanoparticles of radius  $s_1 = 4$  and  $s_2 = 1$ .

is made up of an exponential part, for which the results of section 5.2 apply, and an attractive London–van der Waals term treated above. In addition, one needs to take the cut-off  $r^*$  into account. This cut-off is necessary because otherwise, for small enough  $r$ , the Buckingham potential would become negative. Thus, the effective point–nanoparticle potentials are

$$V_0^B(r) = \begin{cases} \infty & \text{if } r < s + r^* \\ \frac{a}{b^3} V_0^E(br, bs) - cV_0^6(r) & \text{if } r > s + r^* \end{cases} \quad (85)$$

$$V_h^B(r) = \begin{cases} \frac{a}{b^2} V_h^E(br, bs) - cV_h^6(r) & \text{if } r < s - r^* \\ \infty & \text{if } |s - r| < r^* \\ \frac{a}{b^2} V_h^E(br, bs) - cV_h^6(r) & \text{if } r > s + r^* \end{cases} \quad (86)$$

while the effective inter-nanoparticle potentials are given by

$$V_{00}^B(r) = \begin{cases} \infty & \text{if } r < D + r^* \\ \frac{a}{b^6} V_{00}^E(br, bs_1, bs_2) - cV_{00}^6(r) & \text{otherwise} \end{cases} \quad (87)$$

$$V_{sh}^B(r) = \begin{cases} \infty & \text{if } -d - r^* < r < D + r^* \\ \frac{a}{b^5} V_{sh}^E(br, bs_1, bs_2) - cV_{sh}^6(r) & \text{otherwise} \end{cases} \quad (88)$$

$$V_{hh}^B(r) = \begin{cases} \infty & \text{if } |d| - r^* < r < D + r^* \\ \frac{a}{b^4} V_{hh}^E(br, bs_1, bs_2) - cV_{hh}^6(r) & \text{otherwise.} \end{cases} \quad (89)$$

While the effective potentials due to the exponential pair potential are different for different cases (no overlap, partial overlap, and complete overlap), because of the presence of a cut-off  $r^*$ , only the non-overlapping case is relevant here.

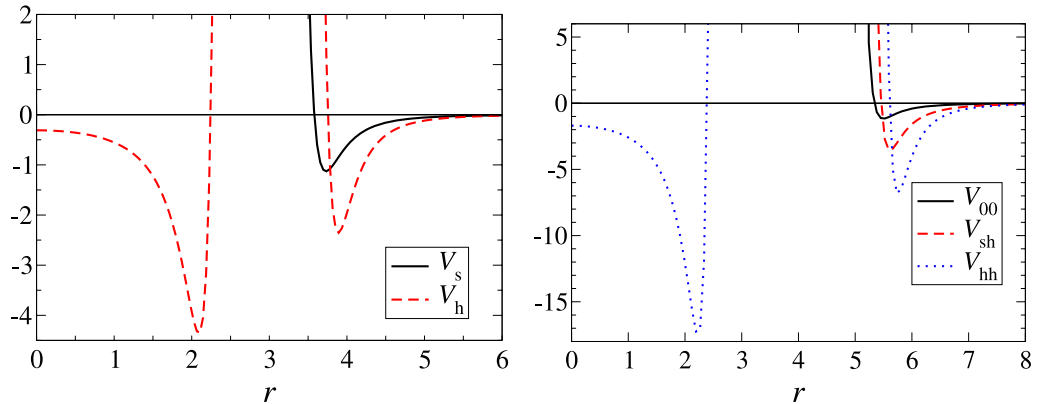


**Figure 7.** Typical example of effective potentials based on the Buckingham potential for  $a = e^{13}$ ,  $b = 13$  and  $c = 2$ , with the cut-off  $r^*$  set to  $1/4$ . The left panel shows the effective potential for a point particle and a solid or hollow nanoparticle of radius  $s = 3$ ; the right panel shows the potentials for two nanoparticles of radius  $s_1 = 4$  and  $s_2 = 1$ .

In figure 7, a typical example of these potentials is shown. Note that while it is possible for a point or nanoparticle particle to be inside the hollow nanoparticle (as long as there is no overlap), there is an infinite barrier to getting inside from the outside, in contrast with the effective potentials based on the Morse potential.

*Lennard-Jones potential.* One of the most often used potentials in molecular dynamics simulations is the Lennard-Jones potential [27], which in reduced units reads

$$\phi^{\text{LJ}}(r) = \frac{1}{r^{12}} - \frac{2}{r^6} = \phi^{12}(r) - 2\phi^6(r). \quad (90)$$

Since the attractive part of the Lennard-Jones potential in equation (90) was handled above, one only needs to add the repulsive part  $r^{-12}$  to find the effective potentials for Lennard-Jones nanoparticles. Substituting  $n = 12$  into the results of section 5.1, and using the relations between auxiliary and effective potentials, one finds

$$V_0^{12}(r) = \frac{4\pi s^3}{3(r^2 - s^2)^6} + \frac{80\pi s^9 + 432\pi r^4 s^5}{45(r^2 - s^2)^9} \quad (91)$$

$$V_h^{12}(r) = \frac{4\pi s^2}{(r^2 - s^2)^6} + \frac{64\pi r^2 s^4 (r^4 + (6/5)s^2 r^2 + s^4)}{(r^2 - s^2)^{10}} \quad (92)$$

$$V_{00}^{12}(r) = \frac{\pi^2}{37800r} \left[ \frac{(r + (7/2)D)^2 + (5/4)D^2 - (15/2)d^2}{(r + D)^7} - \frac{(r + (7/2)d)^2 + (5/4)d^2 - (15/2)D^2}{(r + d)^7} + \frac{(r - (7/2)D)^2 + (5/4)D^2 - (15/2)d^2}{(r - D)^7} - \frac{(r - (7/2)d)^2 + (5/4)d^2 - (15/2)D^2}{(r - d)^7} \right] \quad (93)$$

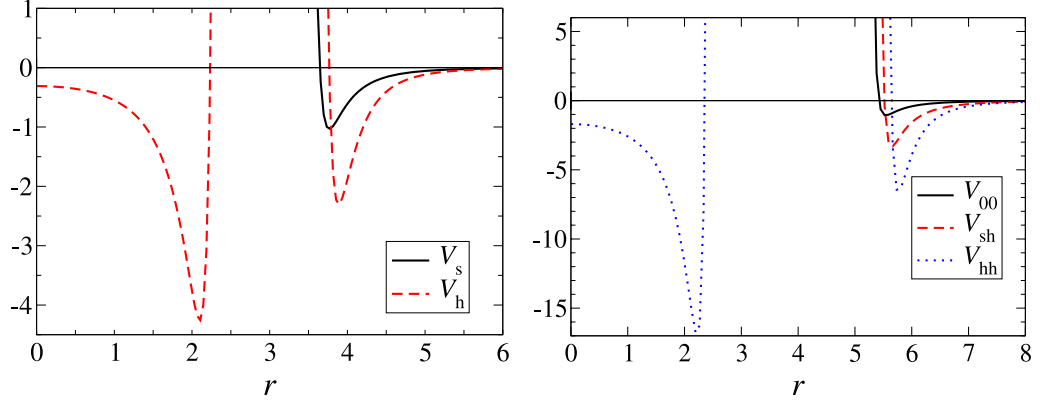


**Figure 8.** Typical effective potentials based on the Lennard-Jones potential (equations (96)–(98)). On the left, the potential for a point particle and solid or hollow nanoparticle of radius  $s = 3$  is shown, and on the right, the potentials for two nanoparticles of radius  $s_1 = 4$  and  $s_2 = 1$ .

$$V_{sh}^{12}(r) = \frac{\pi^2 s_2}{1260r} \left[ -\frac{r + (9/2)D + (7/2)d}{(r+D)^8} - \frac{r - (9/2)D - (7/2)d}{(r-D)^8} + \frac{r + (9/2)d + (7/2)D}{(r+d)^8} + \frac{r - (9/2)d - (7/2)D}{(r-d)^8} \right] \quad (94)$$

$$V_{hh}^{12}(r) = \frac{2\pi^2 s_1 s_2}{45r} \left[ \frac{1}{(r+D)^9} + \frac{1}{(r-D)^9} - \frac{1}{(r+d)^9} - \frac{1}{(r-d)^9} \right]. \quad (95)$$

The potential  $V_{00}^{12}$  is in agreement with the result in the appendix of [1]. The point-nanoparticle potentials for the Lennard-Jones potential are now given by

$$V_0^{LJ}(r) = V_0^{12}(r) - 2V_0^6(r) = \frac{4\pi s^3}{3(r^2 - s^2)^6} + \frac{80\pi s^9 + 432\pi r^4 s^5}{45(r^2 - s^2)^9} - \frac{8\pi s^3}{3(r^2 - s^2)^3} \quad (96)$$

$$V_h^{LJ}(r) = V_h^{12}(r) - 2V_h^6(r) = \frac{4\pi s^2}{(r^2 - s^2)^6} + \frac{64\pi r^2 s^4 (r^4 + (6/5)s^2 r^2 + s^4)}{(r^2 - s^2)^{10}} - \frac{8\pi s^2}{(r^2 - s^2)^3} - \frac{16\pi s^4}{(r^2 - s^2)^4}. \quad (97)$$

Equation (96) gives in more concise notation the result of Roth and Balasubramanya (equation (2) in [15]). Likewise, the inter-nanoparticle interactions due to a Lennard-Jones potential are given by

$$V_{ij}^{LJ}(r) = V_{ij}^{12}(r) - 2V_{ij}^6(r), \quad (98)$$

where  $ij = 00, sh$  or  $hh$ . In figure 8, a typical example of these effective potentials is shown. Note the hard core part of the potentials. For the specific case of a system of nanoparticles with the same radii  $s_1 = s_2 = s$ , studied in [28], the effective

**Table 1.** Coefficients for the polynomials appearing in the effective inter-nanoparticle potentials based on the Lennard-Jones potentials, i.e.,  $V_{00}^{\text{LJ}}$ ,  $V_{\text{sh}}^{\text{LJ}}$  and  $V_{\text{hh}}^{\text{LJ}}$  in equations (99)–(101).

$i$	0	1	2	3	4	5	6	7	8
$\alpha_i^{\text{ss}}$	$-\frac{2^{13}}{315}$	$\frac{219\,136}{4725}$	$-\frac{24\,064}{675}$	$\frac{3456}{225}$	$-\frac{2^7}{45}$	$\frac{2^4}{9}$			
$\alpha_i^{\text{sh}}$	$\frac{2^{15}}{315}$	$-\frac{2^{16}}{315}$	$\frac{2^{13}}{45}$	$-\frac{2^{12}}{45}$	$\frac{2^7}{3}$	$-\frac{2^8}{15}$	$\frac{2^4}{3}$		
$\alpha_i^{\text{hh}}$	$\frac{2^{20}}{45}$	$-\frac{2^{18}}{5}$	$\frac{2^{18}}{5}$	$-\frac{917\,504}{30}$	$\frac{57\,344}{5}$	$-\frac{13\,312}{5}$	$\frac{14\,336}{15}$	$2^7$	$2^4$

inter-nanoparticle interactions can be written in terms of  $\eta = r/s$  as

$$V_{00}^{\text{LJ}}(r) = \frac{\pi^2 \sum_{i=0}^5 \alpha_i^{\text{ss}} \eta^{2i}}{s^6 \eta^8 (\eta^2 - 4)^7} - \frac{4\pi^2}{3} \frac{\eta^2 - 2}{\eta^2 (\eta^2 - 4)} - \frac{\pi^2}{3} \ln \left( 1 - \frac{4}{\eta^2} \right) \quad (99)$$

$$V_{\text{sh}}^{\text{LJ}}(r) = \frac{\pi^2 \sum_{i=0}^6 \alpha_i^{\text{sh}} \eta^{2i}}{s^7 \eta^8 (\eta^2 - 4)^8} - \frac{32\pi^2}{3s \eta^2 (\eta^2 - 4)^2} \quad (100)$$

$$V_{\text{hh}}^{\text{LJ}}(r) = \frac{\pi^2 \sum_{i=0}^8 \alpha_i^{\text{hh}} \eta^{2i}}{s^8 \eta^{10} (\eta^2 - 4)^9} - 32\pi^2 \frac{\eta^4 + 6\eta^2 - 8}{s^2 \eta^4 (\eta^2 - 4)^3} \quad (101)$$

with the  $\alpha$  coefficients given in table 1. Equation (101) is the so-called Girifalco potential [21].

## 6. Accuracy of Lennard-Jones-based potentials for fcc nanoparticles

Since the effective potentials derived above are intended to model nanoparticles, it is natural to ask to what extent they can represent the interactions of nanoclusters composed of discrete atoms. The answer will obviously depend on the structure of the nanoclusters, but to get at least a partial answer, the fcc nanoparticles introduced in section 2 will be used again, with the basic pair potentials  $\phi_{\text{pn}}$  and  $\phi_{\text{nn}}$  given by the Lennard-Jones potential  $\phi^{\text{LJ}}$  in equation (90). The Lennard-Jones potential has a minimum at  $r = 1$ , which sets the unit of length. The fcc nanoparticles are constructed from an fcc lattice with mean density  $\bar{\rho} = 1$  by picking an atom and including all atoms within a given distance from it. Note that this gives only specific values for the number  $M$  of included atoms, since many atoms lie at the same distance in the crystal structure.  $M$  was restricted to being less than 20 000, resulting in 206 clusters, the largest of which has  $M = 19\,861$  atoms.

The mean density  $\bar{\rho} = 1$  for the fcc nanoparticles is not unrealistic: it results in a lattice distance  $a = 4^{1/3}$  ([22], p 12), i.e., the ratio of the lattice distance to the interaction range is  $4^{1/3} \approx 1.587$ . A comparable ratio is found in the case of platinum nanoparticles in water: assuming that the lattice distance  $a$  is the same as in a bulk platinum crystal,  $a = 3.92 \text{ \AA}$  ([22], p 23), and using that the range of interaction of Pt atoms with water is of the order of 2–3  $\text{\AA}$  (see e.g. [32]), one finds a ratio of  $3.92 \text{ \AA} / 2.5 \text{ \AA} = 1.568$ .

To test the applicability of describing these fcc nanoclusters as spheres with a constant density, one should compare the effective point–nanoparticle potential  $V_{\text{pn}} = \rho V_0^{\text{LJ}}$  to the result of summing the potentials  $\phi^{\text{LJ}}$  between the point particle and each of the atoms in the fcc nanoparticle. Similarly, the effective potential  $V_{\text{nn}} = \rho^2 V_{00}^{\text{LJ}}$  between two equally

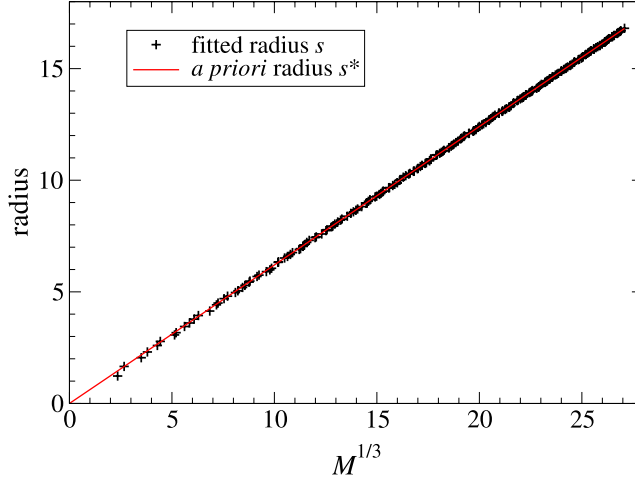


**Figure 9.** Comparison of the fitted radius  $s$  and the *a priori* radius  $s^*$  of the fcc nanoparticles, as a function of the cube root of the number of atoms  $M$  in the nanoparticles. The fit is based on minimizing  $\tilde{\Delta}_{\text{pn}}(s)$ , but minimizing  $\tilde{\Delta}_{\text{nn}}(s)$  instead gives indistinguishable results.

sized nanoparticles should be compared to the result of summing the potentials between each of the atoms of one of the nanoparticles and each of the atoms in the other.

However, there are two difficulties in performing these comparisons. First, the effective potentials are spherically symmetric, but the summed potentials will not be, since the fcc nanoparticles are not truly spherically symmetric. Therefore, the comparison will be made with the summed potentials averaged over all orientations of the nanoparticles, which will be denoted by  $V_{\text{pn}}^{\text{sum}}$  and  $V_{\text{nn}}^{\text{sum}}$ .

The second problem with the comparison is that the radius  $s$  of the nanoparticle, which enters as a parameter in the effective potentials, is not well defined. A reasonable *a priori* radius would be  $s^* = [3M/(4\pi\rho)]^{1/3}$ , but other values for the radius  $s$  close to  $s^*$  are just as reasonable. Thus, the radius may be viewed as a fitting parameter, which will be adjusted to minimize the difference between the effective and the summed potential. To be precise, the following quantities are minimized by varying  $s$ :

$$\begin{aligned}\tilde{\Delta}_{\text{pn}} &= \left\{ \int' dr [V_{\text{pn}}^{\text{sum}}(r) - \rho(s)V_0^{\text{LJ}}(r)]^2 \right\}^{1/2} \\ \tilde{\Delta}_{\text{nn}} &= \left\{ \int' dr [V_{\text{nn}}^{\text{sum}}(r) - \rho^2(s)V_{00}^{\text{LJ}}(r)]^2 \right\}^{1/2}.\end{aligned}\quad (102)$$

Here,  $\rho(s) = 3M/(4\pi s^3)$ , and the prime denotes the restriction on the integration that  $V_{\text{pn}}^{\text{sum}}(r) < 3V_{\text{pn}}^*$  or  $V_{\text{nn}}^{\text{sum}}(r) < 3V_{\text{nn}}^*$ , respectively, where  $V_{\text{pn}}^*$  and  $V_{\text{nn}}^*$  are the absolute values of the minima of  $V_{\text{pn}}^{\text{sum}}$  and  $V_{\text{nn}}^{\text{sum}}$ . These restrictions are needed to make the integrals converge, but the results depend very little on the precise choice of the restriction. For instance, changing the restriction to  $2V^*$  instead of  $3V^*$  shifts the values for the radii  $s$  only by an amount of the order of  $10^{-4}$ .

The values of the radius that result from minimizing  $\tilde{\Delta}_{\text{pn}}$  for the 206 cluster configurations with  $M < 20\,000$  are shown in figure 9. It is seen that except for some

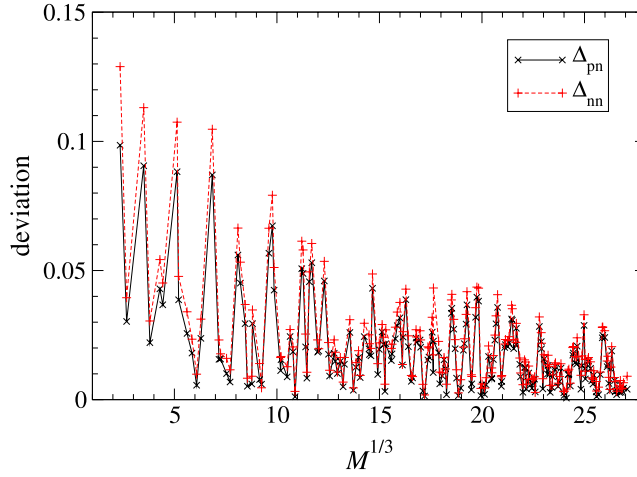


**Figure 10.** Deviations  $\Delta_{\text{pn}}$  and  $\Delta_{\text{nn}}$  of the effective potentials from the atom-by-atom summed potentials for the fcc nanoparticles as a function of the cube root of the number of atoms  $M$  in the cluster.

of the smaller clusters, the values of fitted radii  $s$  typically lie very close to the *a priori* radius  $s^*$ . Minimizing  $\tilde{\Delta}_{\text{nn}}$  instead results in the same values for the radii to within 0.3%.

To get an idea of the accuracy of the fits as a function of nanoparticle size, one may investigate the values of the dimensionless deviations

$$\Delta_{\text{pn}} = \frac{\tilde{\Delta}_{\text{pn}}}{R_{\text{pn}}^{1/2} V_{\text{pn}}^*}; \quad \Delta_{\text{nn}} = \frac{\tilde{\Delta}_{\text{nn}}}{R_{\text{nn}}^{1/2} V_{\text{nn}}^*}.$$

The length scales  $R_{\text{pn}}$  and  $R_{\text{nn}}$  are chosen as the lengths of the intervals contributing 99.9% of the values of the integrals in equations (102). This construction of  $R_{\text{pn}}$  and  $R_{\text{nn}}$  typically gives  $R_{\text{pn}} \approx 1.35$  and  $R_{\text{nn}} \approx 2$  for the size of clusters investigated here, and for simplicity, these values of  $R_{\text{pn}}$  and  $R_{\text{nn}}$  were used for all clusters. The dimensionless deviations are plotted in figure 10. One sees a high degree of correlation between the accuracy of the effective potential for a nanoparticle and point particle and the accuracy of the effective potential between two nanoparticles. The deviations are furthermore typically small, indicating that there is good agreement between the effective potentials and the sum of atom–atom potentials, although the deviations are larger for specific cluster sizes. According to figure 10, for nanoparticles of a size  $M$  greater than about  $12^3$ , using the effective potentials leads to deviations less than 5%. To get an idea of the physical order of magnitude, using units borrowed from silver nanoparticles (see above), one sees that nanoparticles of this size have a diameter of about 10 nm, which seems a physically plausible lower limit of the applicability of the effective potentials.

As extreme examples, figure 11 shows a case of very good agreement and figure 12 shows a case of poorer agreement. In these figures, the effective potentials and the summed potentials are compared for  $M = 18\,053$  with  $s = 16.27$  and  $M = 17\,357$  with  $s = 16.04$ , respectively. Note that the agreement is never very bad, but for the latter, the depth of the minimum is somewhat underestimated by the effective potentials, as the insets of figure 12 show.

Effective pair potentials for spherical nanoparticles

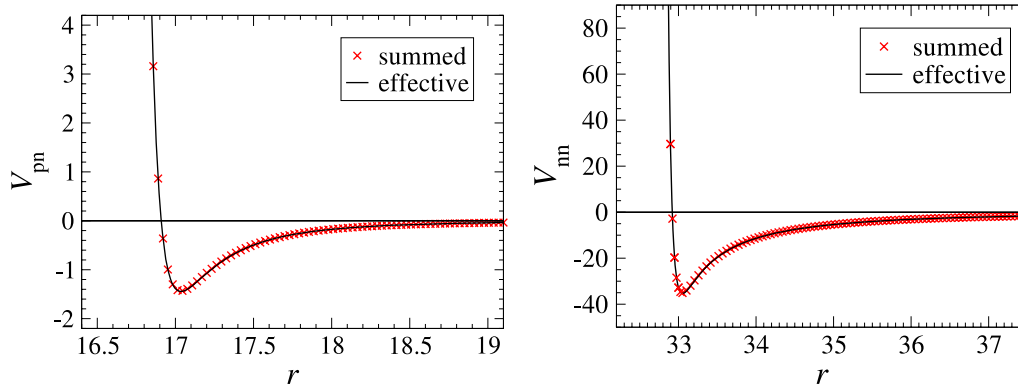


**Figure 11.** An example of very good agreement between the effective and summed potentials, which occurs for an fcc nanocluster of size  $M = 18\,053$  with an effective radius of 16.27 (in dimensionless units). Crosses represent the orientationally averaged summed potentials  $V_{pn}^{\text{sum}}$  (left) and  $V_{nn}^{\text{sum}}$  (right), while the solid lines are the effective potentials  $V_{pn} = \rho V_0^{\text{LJ}}$  (left) and  $V_{nn} = \rho^2 V_{00}^{\text{LJ}}$  (right).

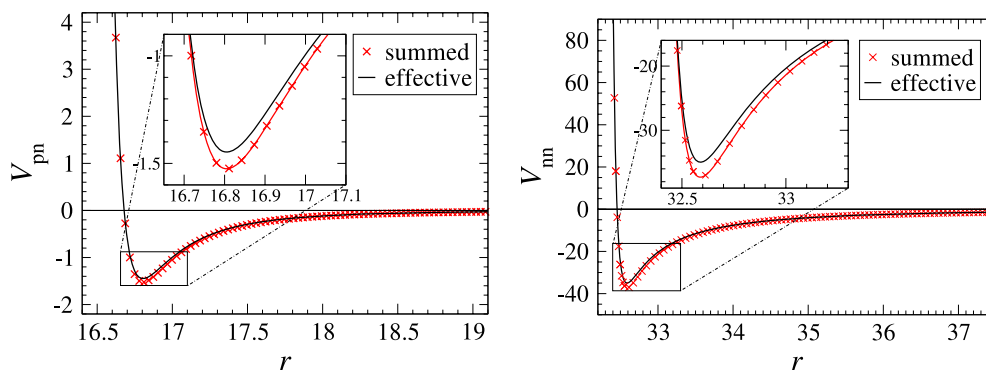


**Figure 12.** An example of poorer agreement between the effective and summed potentials, which occurs for an fcc nanocluster of size  $M = 17\,357$  with an effective radius of 16.04 (dimensionless units). Solid lines represent the effective potentials  $V_{pn} = \rho V_0^{\text{LJ}}$  (left) and  $V_{nn} = \rho^2 V_{00}^{\text{LJ}}$  (right), while crosses are the orientationally averaged summed potentials  $V_{pn}^{\text{sum}}$  (left) and  $V_{nn}^{\text{sum}}$  (right). The insets zoom in on the minima of the potentials, and show that their depths are underestimated by the effective potentials.

It is hard to say in general why the smooth, constant density description works better for some clusters than for others. For some of the smaller nanoclusters with poorer agreement, inspecting the spatial structure of the nanocluster shows a rather rough surface, which could be the explanation. But for the larger nanoparticles, such differences in roughness are hard to distinguish.

## 7. Discussion

A general effective description for rigid nanoparticles was presented, starting from a smoothing procedure in which the real spatial density profile inside the nanoparticles

is replaced by a spherically symmetric one. The resulting effective interactions between a nanoparticle and a point particle as well as between two nanoparticles are then given by spherically symmetric potentials, thus greatly simplifying the description over an all-atom model.

The main results of this approach are the formulations of the effective potentials in terms of auxiliary potentials, equations (17) and (18), which tend to have a simpler form than the full effective potential and which furthermore provide a unified description of overlapping and non-overlapping configurations. While the latter is usually the only physical situation, overlap can occur for instance for hollow nanoparticles containing other smaller particles. The auxiliary potentials are related to the basic interaction potentials through equations (19) and (20). Furthermore, the effective potentials for hollow particles were found to be related to those for solid nanoparticles by simple differentiation with respect to the radii of the nanoparticles (see equations (47) and (50)), and as such also allow a formulation in terms of auxiliary potentials (see section 4).

It should be realized that elastic effects are thrown out of the description by assuming rigidity of nanoparticles. Rigidity of nanoparticles is not an uncommon assumption (see e.g. [1, 5], [14]–[16], [20] and [21]), but of course, there are physical situations in which this assumption is not appropriate, especially at higher energies.

As an application of the formalism, explicit effective pair potentials for solid and hollow nanoparticles were obtained for various basic pair potentials. Different pair potentials have different applications. For instance, the Lennard-Jones potential is a general-purpose potential, while the Buckingham potential is suited to describe the physics of particles close together such as in high pressure systems. These basic potentials result in effective nanoparticle potentials with hard cores plus a soft potential. They reduce in limiting cases to some of the existing model potentials for colloids, such as that of hard spheres and the Hamaker potential [20, 23, 11], but not to more ad hoc models such as the description of a colloid as a single big Lennard-Jones particle [24], shifted Lennard-Jones potentials [7], and variants thereof [25]. In contrast, the Morse potential is able to describe bounded systems or penetrable particles, making it possible to model nanoparticles that could passively capture and trap specific types of particles. The resulting effective potentials could have applications in modeling drug delivery by (hollow) nanoparticles [9] and viral capsids [10].

For the case of a Lennard-Jones basic potential, a comparison was carried out with an atomic model of a nanocluster. In this model, the atoms making up the nanoparticle were assumed to be arranged in an fcc lattice structure. To find approximate spherical structures, the atoms were restricted to lying within a certain distance from the central atom in the nanocluster. Configurations with up to 19861 atoms were studied. The effective potentials were compared with the orientationally averaged sum of Lennard-Jones potentials due to the individual atoms. The agreement tends to be very good, provided the radius in the effective description is treated as a fitting parameter. For some configurations, however, the fitting procedure underestimates the depth of the minimum of the potentials. The shallower depth may be due to surface roughness of these structures, which is caused by the imposed fcc structure and unlikely to be relevant for real nanoclusters.

The application of the explicit expressions for the effective potentials in numerical studies of spherical nanoparticles is in principle straightforward. In fact, the potentials

in equations (96) and (99) have already been used in a numerical study of single-particle transport in an equilibrium nanofluid composed of solid nanoparticles and fluid particles interacting through Lennard-Jones interactions, where the validity of a Gaussian approximation to the Van Hove self-correlation function was investigated, and found to hold up to picosecond timescales for the fluid particles, and up to 5–10 times longer (depending on temperature) for nanoparticles with a size of about 2 nm [28].

Given the explicit expressions for the effective potentials, the description allows a fairly direct route toward a qualitative model for a given system of nanoparticles in a fluid, since reasonable values for the parameters for commonly used pair potentials are available in the literature [33], while the number of atoms in a nanoparticle and its radius could be taken from experiments or theoretical calculations [12]. Furthermore, the effective potentials have a physical range based on the interaction of their constituents rather than on their radius. Therefore, the effective potentials that were derived here are expected to be useful for the qualitative description of a wide variety of systems, from mono-disperse nanoparticles in a fluid to mixtures of different kinds of fluid particles, nanoclusters or buckyballs.

A number of interesting extensions present themselves for future research. For instance, while the nanoparticles were assumed to be composed of one kind of particle only, potentials for nanoparticles composed of several kinds of particles can also be derived within the current context if the distribution of the kinds is either homogeneously mixed or distributed in spherical shells (so-called core-shell nanoparticles [6, 34]). The spherical symmetry of the effective potentials, which decouples the rotational and translational degrees of freedom, could be lifted to extend the model to include rotational motion. For specific cases, effective potentials can still be found through integration [17]–[19]. In general, the extension to non-spherical objects may be accomplished by adding interaction sites on the surface of the nanoparticle or a multipole expansion. As long as the orientationally dependent potential is available, there are no obstacles in molecular dynamics simulations of such systems [35]. Furthermore, combining the current model with the mesoscopic fluid model of Malevanets and Kapral [36] would yield a numerically efficient model of larger nanoparticles and colloids that includes hydrodynamic effects. These avenues are currently being investigated.

## Acknowledgments

The author wishes to thank Professors E G D Cohen, R Kapral, and J Schofield for useful discussions. Acknowledgment is made to the Donors of the American Chemical Society Petroleum Research Fund for support of this research. This work was furthermore supported by the National Sciences and Engineering Research Council of Canada.

## Appendix. The kernel $K_{ij}$

The integral in the expression for the kernel  $K_{ij}$  in equation (14) will be worked out now. Using equation (9) and the binomial formula for  $(x - y)^{i+2}$ , one finds, after resummation,

that

$$K_{ij}(x, s_1, s_2) = \int_{y_1}^{y_2} dy \frac{4\pi^2\Theta(D - |x|)}{(i+2)(j+2)} [s_1^{i+2} - (x-y)^{i+2}][s_2^{j+2} - y^{j+2}] \quad (\text{A.1})$$

$$= \frac{4\pi^2\Theta(D - |x|)s_1^{i+2}s_2^{j+2}}{(i+2)(j+2)} \left[ y - \frac{s_1}{i+3} \left( \frac{x+y}{s_1} \right)^{i+3} + \frac{s_2}{j+3} \left( \frac{y}{s_2} \right)^{j+3} \left\{ \left( \frac{x}{s_1} \right)^{i+2} F\left(-i-2, j+3; j+4; -\frac{y}{x}\right) - 1 \right\} \right]_{y_1}^{y_2} \quad (\text{A.2})$$

with  $y_1 = \max(-s_2, x-s_1)$  and  $y_2 = \min(s_2, x+s_1)$ , which are due to the finite support for the kernels  $K_i$  and  $K_j$ , and  $F$  is the hypergeometric function [37]. Despite its complicated appearance, equation (A.2) is simply a piecewise polynomial in  $x$  of degree  $i+j+5$  at most. To see this, it is useful to distinguish the following four non-trivial cases: *case 1*:  $x > 0$  and  $|d| < |x| < D$ , for which  $y_1 = x-s_1$  and  $y_2 = s_2$ ; *case 2*:  $d > 0$  and  $|x| < |d|$ , giving  $y_1 = -s_2$  and  $y_2 = s_2$ ; *case 3*:  $d < 0$  and  $|x| < |d|$ , giving  $y_1 = x-s_1$  and  $y_2 = x+s_1$ ; and *case 4*:  $x < 0$  and  $|d| < |x| < D$ , for which  $y_1 = -s_2$  and  $y_2 = x+s_1$ . There are in fact only two independent cases, because *case 3* can be obtained from the result of *case 2* by interchanging  $s_1$  and  $s_2$  as well as  $i$  and  $j$  (which will also flip the sign of  $d$ ), while the result for *case 4* can be obtained from that of *case 1* by setting  $s_1$  to  $-s_2$ ,  $s_2$  to  $-s_1$  and introducing a minus sign, as can be proved by changing the integration variable in equation (A.1) from  $y$  to  $x-y$ . Thus, one only needs to consider *case 1* and *case 2*. Changing the integration variable from  $y$  to  $z = s_2 - y$  and using the binomial formula, equation (A.1) for *case 1* yields

$$K_{ij}(x, s_1, s_2) = (i+2)!(j+2)! \sum_{m=0}^{i+j+2} \frac{(D-x)^{m+3}}{(m+3)!} \times \sum_{k=\max(1, m-j)}^{\min(i+2, m+1)} \frac{(-s_1)^{i+2-k} s_2^{j-m+k}}{(i+2-k)!(j-m+k)!}, \quad (\text{A.3})$$

which is polynomial in  $x$  of degree  $i+j+5$ , while for *case 2* the integral in equation (A.1) can be found by using the binomial formula for  $(x-y)^{i+2}$ , giving a polynomial of degree  $i+2$ , i.e.

$$K_{ij}(x, s_1, s_2) = \frac{8\pi^2 s_2^{j+3}}{i+2} \left[ \frac{s_1^{i+2}}{j+3} - \sum_{k=0}^{i/2+1} \binom{i+2}{2k} \frac{s_2^{i+2-2k} x^{2k}}{(i+3-2k)(i+j+5-2k)} \right]. \quad (\text{A.4})$$

## References

- [1] Schwarz U S and Safran S A, *Phase behavior and material properties of hollow nanoparticles*, 2000 *Phys. Rev. E* **62** 6957
- [2] Choi S U S, Xu X, Koblinski P and Yu W, *Nanofluids can take the heat*, 2002 *Proc. of DOE BES 20th Symp. on Energy Engineering Sciences (Argonne, IL May)*
- [3] Hwang H J, Kwon O-K and Kang J W, *Copper nanocluster diffusion in carbon nanotube*, 2004 *Solid State Commun.* **129** 687
- Tang W and Advani S G, *Drag on a nanotube in uniform liquid argon flow*, 2006 *J. Chem. Phys.* **125** 174706

- [4] Chen X, Samia A C S, Lou Y and Burda C, *Investigation of the crystallization process in 2 nm CdSe quantum dots*, 2005 *J. Am. Chem. Soc.* **127** 4372
- [5] Verberg R, de Schepper I M and Cohen E G D, *Viscosity of colloidal suspensions*, 1997 *Phys. Rev. E* **55** 3143
- [6] Glotzer S C, Solomon M J and Kotov N A, *Self-assembly: from nanoscale to microscale colloids*, 2004 *AIChE J.* **50** 2978
- [7] ten Wolde P R and Frenkel D, *Enhancement of protein crystal nucleation by critical density fluctuations*, 1997 *Science* **277** 1975
- [8] Pellicane G, Costa D and Caccamo C, *Theory and simulation of short-range models of globular protein solutions*, 2004 *J. Phys.: Condens. Matter* **16** S4923
- [9] Jurgons R, Seliger C, Hilpert A, Trahms L, Odenbach S and Alexiou C, *Drug loaded magnetic nanoparticles for cancer therapy*, 2006 *J. Phys.: Condens. Matter* **18** S2893
- Arruebo M, Galán M, Navascués N, Téllez C, Marquina C, Ibarra M R and Santamaría J, *Development of magnetic nanostructured silica-based materials as potential vectors for drug-delivery applications*, 2006 *Chem. Mater.* **18** 1911
- [10] Garcea R L and Gissmann L, *Virus-like particles as vaccines and vessels for the delivery of small molecules*, 2004 *Curr. Opin. Biotechnol.* **15** 513
- [11] Barrat J L and Hansen J P, 2003 *Basic Concepts for Simple and Complex Liquids* (Cambridge: Cambridge University Press)
- [12] Baletto F and Ferrando R, *Structural properties of nanoclusters: energetic, thermodynamic, and kinetic effects*, 2005 *Rev. Mod. Phys.* **77** 371
- [13] Gonzalez Szwacki N, Sadrzadeh A and Yakobson B I, *B<sub>80</sub> fullerene: an ab initio prediction of geometry, stability, and electronic structure*, 2007 *Phys. Rev. Lett.* **98** 166804
- Gopakumar G, Nguyen M T and Ceulemans A, *The boron buckyball has an unexpected T<sub>h</sub> symmetry*, 2008 *Chem. Phys. Lett.* **450** 175
- [14] Bhattacharjee S and Elimelech M, *Surface element integration: a novel technique for evaluation of DLVO interaction between a particle and an infinite flat plate*, 1997 *J. Colloid Interface Sci.* **193** 273
- [15] Roth M W and Balasubramanya M K, *Predicted properties and melting transition of krypton layers physisorbed onto Lennard-Jones spheres*, 2000 *Phys. Rev. B* **62** 17043
- [16] Balasubramanya M K and Roth M W, *Calculated phase boundary including corrugation effects for krypton layers physisorbed onto spherical substrates*, 2001 *Phys. Rev. B* **63** 205425
- [17] Tadmor R, *The London-van der Waals interaction energy between objects of various geometry*, 2001 *J. Phys.: Condens. Matter* **13** L195
- [18] Mahanty J and Ninham B W, 1976 *Dispersion Forces* (London: Academic)
- [19] Israelachvili J N, 1991 *Intermolecular and Surface Forces* 2nd edn (London: Academic)
- [20] Hamaker H C, *The London-van der Waals attraction between spherical particles*, 1937 *Physica* **4** 1058
- [21] Girifalco L A, *Molecular properties of C<sub>60</sub> in the gas and solid phases*, 1992 *J. Phys. Chem.* **96** 858
- [22] Kittel C, 1986 *Introduction to Solid State Physics* 6th edn (New York: Wiley)
- [23] Derjaguin B V and Landau L D, *Theory of stability of highly charged lyophobic sols and adhesion of highly charged particles in solutions of electrolytes*, 1941 *Acta Phys. Chim. USSR* **14** 633
- Verwey E J W and Overbeek J T G, 1948 *Theory of Stability of Lyophobic Colloids* (Amsterdam: Elsevier)
- Cichocki B and Felderhof B U, *Short-time diffusion coefficients and high frequency viscosity of dilute suspensions of spherical Brownian particles*, 1988 *J. Chem. Phys.* **89** 1049
- Cichocki B and Hinsen K, *Dynamics computer simulation of concentrated hard sphere suspensions*, 1990 *Physica A* **166** 473
- [24] Lee S H and Kapral R, *Friction and diffusion of a Brownian particle in a mesoscopic solvent*, 2004 *J. Chem. Phys.* **121** 11163
- [25] Sciortino F, Tartaglia P and Zaccarelli E, *One-dimensional cluster growth and branching gels in colloidal systems with short-ranged depletion attraction and screened electrostatic repulsion*, 2005 *J. Phys. Chem. B* **109** 21942
- de Candia A, Del Gado E, Fierro A, Sator N, Tarzi M and Coniglio A, *Columnar and lamellar phases in attractive colloidal systems*, 2006 *Phys. Rev. E* **74** 010403R
- Fierro A, Del Gado E, de Candia A and Coniglio A, *Dynamical heterogeneities in attractive colloids*, 2008 *J. Stat. Mech.* **L04002**
- Vliegthart G A, Lodge J F M and Lekkerkerker H N W, *Strong, weak and metastable liquids: structural and dynamical aspects of the liquid state*, 1999 *Physica A* **263** 378

- [26] Stephani H, 1990 *General Relativity: an Introduction to the Theory of the Gravitational Field* 2nd edn (Cambridge: Cambridge University Press)
- [27] Lennard-Jones J E, *The equation of state of gases and critical phenomena*, 1937 *Physica* **4** 941
- [28] van Zon R, Ashwin S S and Cohen E G D, *Gaussian approximation to single particle correlations at and below the picosecond scale for Lennard-Jones and nanoparticle fluids*, 2008 *Nonlinearity* **21** R119
- [29] Morse P M, *Diatomic molecules according to the wave mechanics. II. Vibrational levels*, 1929 *Phys. Rev.* **34** 57
- [30] Girifalco L A and Weizer V G, *Application of the Morse potential function to cubic metals*, 1959 *Phys. Rev.* **114** 686
- [31] Buckingham R A, *The classical equation of state of gaseous helium neon and argon*, 1938 *Proc. R. Soc. A* **168** 264
- [32] Spohr E, *Computer simulation of the water/platinum interface*, 1989 *J. Phys. Chem.* **93** 6171
- [33] MacKerell A D Jr *et al*, *All-atom empirical potential for molecular modeling and dynamics studies of proteins*, 1998 *J. Phys. Chem. B* **102** 3586
- [34] Molinero V, Laria D and Kapral R, *Dynamics of solvation-induced structural transitions in mesoscopic binary clusters*, 2000 *Phys. Rev. Lett.* **84** 455
- [35] van Zon R and Schofield J, *Symplectic algorithms for simulations of rigid body systems using the exact solution of free motion*, 2007 *Phys. Rev. E* **75** 056701  
van Zon R, Omelyan I and Schofield J, *Efficient algorithms for rigid body integration using optimized splitting methods and exact free rotational motion*, 2008 *J. Chem. Phys.* **128** 136102
- [36] Malevanets A and Kapral R, *Mesoscopic model for solvent dynamics*, 1999 *J. Chem. Phys.* **110** 8605  
Malevanets A and Kapral R, *Solute molecular dynamics in a mesoscopic solvent*, 2000 *J. Chem. Phys.* **112** 7260
- [37] Gradshteyn I S and Ryzhik I M, 2000 *Table of Integrals, Series, and Products* (San Diego, CA: Academic)